上海交通大學

SHANGHAI JIAO TONG UNIVERSITY

学士学位论文

BACHELOR'S THESIS

论文题目：基于仿生光热界面蒸发的热电化学电池

学生姓名：宁子杨

学生学号：5130519084

专　　业：材料科学与工程

指导教师：邓涛

学院(系)：材料科学与工程学院

基于仿生光热界面蒸发的热电化学电池

摘要

为了维持现代社会的持续发展，解决能源与水资源的短缺，是迫在眉睫的需求。仿生界面蒸发材料，以其卓越的光热转换效率及其产生净水的能力，受到了广泛的关注。当前大多研究都着眼于界面蒸发在海水淡化与水净化的应用，却忽略了界面蒸发过程中所产生的温度梯度也能够被应用于高效率的发电，给能源短缺问题的解决提供新思路。热电化学电池，因为其较高的塞贝克系数，在同样的温场下能够输出电压高于传统半导体热电材料一个数量级的电能，因此被视为在低温差温场中进行高效率发电的较有效的解决方案之一。在本毕业设计中，我将界面蒸发与热电化学电池相结合，实现了基于蒸发过程产生的温度梯度的高效率发电。因为基于I^-/I_3^-氧化还原对的电解质的低成本，低毒性与低温差温场中较好的性能，我将其选用为热电化学体系并引入了 KCl 与α -环糊精以提升其电导率与电压。我采用了不同的方法来提升体系的蒸发效率与热电化学性能，并最终根据蒸发界面温度、开路电压、断路电流等因素选择有多孔聚二甲基硅氧烷进行隔热，利用石墨基还原氧化石墨烯同时作为蒸发界面与电极材料。上述体系在 400mW/cm^2 光照的稳态蒸发下达到了9.44×10^{-3}%的热电转换效率， 高于同种热电化学电池在其他体系中 3×10^{-3}%的热电转换效率。我还提出并验证了一种循环发电的方案，以在实际应用中进行更高效率的发电。本毕业设计的研究为最大化太阳能的转化与利用提供了一种全新的思路。

关键词：热电化学电池，塞贝克效应，仿生界面蒸发，蒸发效率，还原氧化石墨烯，热电转换效率，蒸发隔热

THERMOELECTROCHEMICAL CELL ENABLED BY BIO-INSPIRED INTERFACIAL EVAPORATION

ABSTRACT

Solving the problems of water shortage and energy shortage is an urgent need for the sustainable development of the society. Bio-inspired interfacial evaporation has recently drawn tremendous attention, due to its excellence photothermal conversion efficiency and its demonstrated capability in clean water generation. While most of current researches in this area focus on the applications in water purification and water desalination, there is much less attention on the thermal gradient generated during the interfacial evaporation process, which potential can be used for high-efficient electricity generation and provide another possible solution in dealing with the global energy shortage. Thermal electrochemical cells, with the potential to generate thermoelectric voltage 10x higher than traditional semiconductor materials, can harvest low-grade waste heat and convert it into electricity with considerable efficiency. In this thesis, interfacial evaporation was combined with thermoelectrochemical cell to realize high-efficient electricity generation. The electrolyte based on the redox couple of I^-/I_3^-, with the additional of KCl and α-cyclodextrin (α-CD), has been used in this system, due to its outstanding performance in low-grade thermal gradient, low cost and hypotoxicity. Several strategies have been investigated to optimize both the evaporation efficiency and thermoelectrochemical performance. The system with a bifunctional graphite-based reduced graphene oxide (rGO) and polydimethylsiloxane (PDMS) thermal insulator were fabricated and the surface temperature, open-circuit voltage and short-circuit current were characterized. The maximum energy conversion efficiency of $9.44 \times$

10^{-3}% has been achieved with the above system under the solar radiation of 400mW/cm^2. At the end of the thesis a scheme with cyclic electricity generation that can maintain a higher voltage level and harvest heat more efficiently is proposed for scalable application in practice. Such a demonstration should open up a new strategy for maximizing solar energy conversion and utilization.

Key words: Thermoelectrochemical cell, Seebeck Coefficient, Bio-inspired interfacial evaporation, Evaporation efficiency, Reduced graphene oxide, thermal insulation, Heat harvesting

Contents

Chapter One Introduction

With rapid increase of world population and global expansion of industries, energy shortage and lack of drinkable water have been the biggest problems in modern times. While the exhaustion of fossil fuels are predicted in the very near future, renewable energy resources seem to be the only choice to sustain the development of society([1], Boyle, 1997, [2], Hoffert, et al., 2002: 981-987, [3], Johansson, 1993, [4], Turner, 1999: 687-689.), without leading to severe environmental pollution and global warming. The solar energy, for its massive amount and relatively stable output power, is considered as the most reliable one among renewable energy resources. With the help of bio-inspired photothermal materials, solar energy can be converted into thermal energy in considerable efficiency. By localizing the solar energy at the evaporation surface, high-performance large-scale evaporation can be achieved for sea water desalination, which can potentially relieve the global lack of drinkable water([5], Cartlidge, 2011: 922-4, [6], Elimelech and Phillip, 2011: 669-671 [7], Gupta and Kaushik, 2010: 1228-1235, [8], Scuderi, et al., 2014: 11189-11195.). Due to the multifunctional property of interfacial evaporation materials, such as reduced graphene oxide (rGO) with coating of TiO_2, pollutant inside the water can be decomposed and absorbed during evaporation, which can in the meantime, relieves the industrial pollution.

With Herculean effort of many research groups on bio-inspired interfacial evaporation, the photothermal efficiency has been raised to extremely high level, which almost achieves the theoretical limit. However, while focusing on transferring the energy from solar radiation to water, many researchers ignore that a great amount of heat has been wasted during the evaporation, which can be made use of for electricity generation. The waste heat has, so far, be harvested through many indirect methods,

including driving ionic solution([9], Fh, et al., 2007: 1022-1025.), electro kinetic effect([10], Li, et al., 2017: 81-86, 11], Xue, et al., 2017: 317-321.) and coupling of ions sustained by water flow([12], Dhiman, et al., 2011: 3123-3127.). Another method of heat harvesting with higher efficiency is through thermoelectrochemical cell, which allows the difference in temperature to be converted directly into electricity with no moving parts. The thermoelectrochemical cell relies on the electrochemical Seebeck Effect, in which the thermal gradient leads to different redox reactions at the hot side and cold side of the cell. Different reactions at two sides cause a difference in their electrochemical potentials, thus flow of current can be generated with a closed circuit.

The bio-inspired interfacial evaporation and thermoelectrochemical cell are indeed a perfect match. The key factor in interfacial evaporation is heat localization. By localizing the heat at the surface of the system, water at the surface can be converted into vapor at a high speed, without heating up the whole bulk volume of water in the system. The sharp thermal gradient from the top to the bottom, formed by heat localization is beneficial to thermoelectrochemical cell, since the larger the temperature difference between two sides, the higher the voltage and efficiency can be achieved through Seebeck Effect.

To assure the outstanding performance of water desalination and electricity generation as well as the possibility of scalable application, suitable combinations of interfacial evaporation system and thermoelectrochemical cell must be chosen among all the candidate materials.

1.1Bio-inspired interfacial evaporation materials

Currently, steam generation by solar radiation is based on heating up the whole bulk water with extremely high light intensity. Such method requires costly equipment to

concentrate the solar radiation to a great extent, and leads to severe heat loss into the environment due to the hot bulk liquid. The ideal steam generation method should be sustained in regular solar radiation, without heating up the bulk liquid. The plant leaf has set a great example of evaporation—during transpiration, only water at the surface of the leaf, rather than the bulk water is heated up and evaporated continuously and efficiently. The bio-inspired interfacial evaporation materials can localize the heat at the surface by high-efficient photothermal conversion to form high temperature at specific area, leading to continuous evaporation at the surface of the system, thus minimizing the heat loss and improve the evaporation efficiency.

The interfacial evaporation materials can be divided into two different types. The first type relies on surface plasmon resonance to converse solar energy into heat with high efficiency, while the second relies on the intrinsic solar absorption of materials to absorb as much solar energy from radiation as possible.

1.1.1 Interfacial evaporation based on surface plasmon resonance

Surface Plasmon Resonance (SPR) is the resonant oscillation of conduction electrons at the interface between negative and positive permittivity material stimulated by incident light. In the resonant state, the energy of electromagnetic wave has been efficiently converted into kinetic energy of oscillating electrons at the surface, through which the solar energy can be effectively converted into heat.

Since Au nanoparticles (AuNP) have the characteristic of surface plasmon resonance, membrane of AuNP has been employed by many researchers as the interfacial evaporation materials. Using surface plasmon resonance to enhance the rate of photothermal conversion, Zhenhui Wang's research([13], Wang, et al., 2014: 3234-3239.) on free-floating film of gold nanoparticles has reached a light-to-heat

conversion efficiency of 44% during the evaporation at the air-water interface. Yanming Liu et al.([14], Liu, et al., 2015: 2768-2774.) have demonstrated that the membrane of AuNP assembled on airlaid paper can reach a conversion rate of 77.8%. Such airlaid-paper based membrane is portable and capable of being cycled for more than 30times. Multiple-layered structure of AuNP membrane and TiO_2 has also been fabricated as bifunctional evaporation surface([15], Liu, et al., 2016: 772-779.) for water purification and clean water generation.

Lin Zhou's research([16], Zhou, et al., 2016: .) reveals that aluminium has a higher plasma frequency than gold and silver, thus is expected to result in a significant plasmonic response in UV regime. With the plasmonic structure of Al nanoparticles and anodic aluminium oxide membrane, a steam generation efficiency of 88.4% can be reached under the solar radiation of 4 suns (400mW/cm^2).

Besides, Lin Zhou's research([17], Zhou, et al., 2016: e1501227.) on multiple plasmonic system has broadened the bandwidth of solar absorption, thus enhances the steam generation efficiency. By developing a template-assisted physical vapor deposition (PVD) process, random-sized, widely anisotropic-shaped gold nanoparticles have been deposited on the template by self-assembly. The alumina template, with pore size between 30 to 400nm, is fabricated by anodization process. This multiple plasmonic solar absorber, succeeded in achieving high density of optical modes, strong internal reflection and relatively low refractive index, affording a steam generation efficiency of more than 90% under the solar radiation of 400mW/cm^2.

However, since surface plasmon resonance only works at the surface of gold, silver and aluminium, the cost and complexity of the membrane synthesis has limited its scalable application.

1.1.2 Interfacial evaporation based on intrinsic solar absorption

Surfaces contain other types of materials such as carbon black or graphene, have been employed as evaporation surface, due to their outstanding absorption performance in a wide range of radiation spectrum. Based on their wide absorption spectrum, greater amount of the solar energy has been converted into heat at the surface, which leads to heat localization for interfacial evaporation.

Reduced graphene oxide (rGO) has been demonstrated by Jinwei([18], Lou, et al., 2016: 14628-14636.) to have a wide absorption spectrum and high photothermal efficiency as evaporation surface. In the meantime, due to the porosity of rGO, it is also capable of decomposing and absorbing the pollutants for water purification. Graphite, in the meantime, is also reported to have perfect absorption spectrum, especially the foliated graphite. According to Ghasemi's research([19], Ghasemi, et al., 2014: 4449-4455.), foliated graphite can absorb 97% of all the solar power as evaporation surface. In the meantime, since the foliated graphite flakes has surface area, 32 times larger than that of ordinary graphite flakes, it can transfer heat from the evaporation surface to the fluid more effectively.

Xiaozhen Hu's work([20], Hu, et al., 2017: .) on graphene oxide (GO)-based aerogels, has revealed its potential as an ideal type of evaporation surface with carefully tailored absorption as well as thermal and hydrophilic properties. The RGO-SA-CNT aerogel is free-floating and has perfect hydrophilicity and porous networks, which can be applied for water supply and vapor channels. The RGO-SA-CNT aerogel has also enhanced thermal localization due to its thermal insulating property. A steam generation efficiency of 83% can be achieved under the solar radiation of 4 sun ($400mW/cm^2$).

Interfacial evaporation materials based on intrinsic solar absorption is usually based on carbon compound. Compared to plasmonic solar absorber, they are easily

synthesized and with low-cost. More importantly, due to the porous structure of carbon compounds, perfect hydrophilicity and thermal insulation can be achieved in the meantime, which are definitely crucial to improve the efficiency of interfacial evaporation.

1.1.3 Efficiency calculation of interfacial evaporation

Calculation of the efficiency for steam generation is pre-requisite for the comparison of different evaporation surface materials. By calculating true efficiency of different evaporation surface, we can, accordingly, determine the system with the best performance. We herein adopt the equation (1-1) proposed by Chen's Group([19], Ghasemi, et al., 2014: 4449.) to calculate the evaporation efficiency, which is also known as light-to-heat conversion efficiency.

$$\eta_{th} = \frac{\dot{m} h_{LV}}{C_{opt} q_i} \tag{1-1}$$

In this equation, $\dot{m}$ denotes the mass flux during evaporation, h_{LV} is the total enthalpy of liquid to vapor phase change, which is combined of sensible heat and phase-change enthalpy. C_{opt} is the optical concentration and q_i is the nominal direct solar irradiation of 100mW/cm^2.

In this work, all of the experiments are carried with the solar radiation of 400mW/cm^2, thus the optical concentration is 4. Mass flux during evaporation is calculated by linear fitting of the mass data collected by electronic balance and selecting the slope of mass change at steady state. h_{LV}, the enthalpy change of liquid to vapor phase change, consists the sensible heat and the phase-change enthalpy. The amount of sensible heat is determined by the temperature of generated vapor. In our work, the vapor temperature is treated the same as evaporation surface. A higher evaporation

efficiency can, therefore, be achieved by forming an evaporation surface of higher temperature by heat localization.

1.2Thermoelectrochemical cell

Heat harvesting has drawn great attention due to the rapidly growing need of energy resources. Currently, solid state semiconductor thermoelectric devices have dominated practical application due to the direct conversion of heat to electricity, in spite of low efficiency and high cost. Although many advances have been made, we are still suffering from the absence of efficient, inexpensive devices that are able to convert the low-grade waster heat into electricity. At this time, thermoelectrochemical cells based on different redox couples have been investigated for the lower-cost and outstanding Seebeck Coefficient, especially under low-grade circumstances. With different redox half-reactions happening at hot and cold sides of the device([21], Hertz and Ratkje, 1989: 1698-1704.), electric potential difference can be achieved, thus forms the current flow with complete circuit. Major types of redox couples that have been brought into practical application include $Fe(CN)_3/Fe(CN)_6$, I^-/I_3^- and Co^{II}/Co^{III}. Comparison of low-grade Seebeck Coefficient, poisonousness and cost of different electrolyte should be made to reveal the redox couple that best fits the experimental condition during evaporation.

1.2.1 Thermoelectrochemical cell based on $Fe(CN)_3/Fe(CN)_6$

Despite toxicity, the redox couple of $Fe(CN)_3/Fe(CN)_6$ have been widely investigated for its stability and outstanding Seebeck Coefficient([22], Hu, et al., 2010: 838-846, [23], Kang, et al., 2012: 477–489.). The reaction process inside the cell is as follow:

$$(Hot\ Anode)\ Fe(CN)_6^{4-} - e = Fe(CN)_6^{3-} | Fe(CN)_6^{3-} + e = Fe(CN)_6^{4-}\ (Cold\ Cathode)$$

The oxidation of $Fe(CN)_6^{4-}$ happens on the anode at the hot side, while the reduction of $Fe(CN)_6^{3-}$ happens on the cathode at the cold side. Based on the different electrochemical potentials of half-reactions, the flow of electrons can be formed with complete circuit. Unlike normal electrochemical batteries, the oxidation and reduction reactions happen in the same solution without separator, where reactants and products can diffuse to both sides as reaction continues. The voltage herein is merely based on different reactions at two sides of thermal gradient without changing the components of electrolyte, so the voltage and current are sustainable, as long as the thermal gradient remains.

Weijin Qian has demonstrated that 0.4M $Fe(CN)_3/Fe(CN)_6$ solution has the best performance, with a Seebeck Coefficient of 1.42mV/K([24], Qian, et al., 2016: 240-246.). Advances of this thermoelectrochemical cell has also been made to enhance the current and electrochemical efficiency by applying porous carbon nanotube as electrode materials to enlarge the specific surface area.

1.2.2 Thermoelectrochemical cell based on $Co^{II/III}$tris(bipyridyl)

Ionic liquid electrolyte was first introduced as thermoelectrochemical electrolyte by Abraham in 2013([25], Abraham, et al., 2013: 2639-2646.), which breaks the temperature limit of the boiling point of water at the hot side. Although higher voltage can be achieved with higher temperature difference between the hot and cold sides, the thermoelectrochemical cell would be no longer sustainable, once the evaporation of electrolyte happened. In this case, the boiling point of more than 100℃ of the ionic liquid electrolyte makes it feasible in environment of higher temperature. In this ionic liquid electrolyte, $Co^{II/III}$tris(bipyridyl) has been employed as a redox couple with

outstanding performance under circumstances between 100-200℃. The electrolyte of $Co^{II}/^{III}$tris(bipyridyl) has a larger entropy change in redox reaction than other electrolyte, thus has a higher rate of energy conversion and higher Seebeck Coefficient([26], Lazar, et al., 2016: 1404-10.). In different types of ionic electrolyte with different concentrations, the $Co^{II}/^{III}$tris(bipyridyl) redox couple can reache a Seebeck Coefficient between 1.5-2.2mV/K, and the maximum was achieved in 0.01M 3-methoxypropionitrile (MPN).

$$(Hot\ Anode)\ Co^{2+} - e^- = Co^{3+} | Co^{3+} + e^- = Co^{2+}\ (Cold\ Cathode)$$

Due to the thermal stability of both $Co^{II}/^{III}$tris(bipyridyl) and ionic liquid, it can be applied under high temperature condition. The combination has been employed for heat harvesting, when the temperature at hot side is between 100-200℃, due to the better performance than other redox couples in hot temperature

1.2.3 Thermoelectrochemical cell based on I^-/I_3^-

The mechanism of thermoelectrochemical cell based on redox couple of I^-/I_3^- can be easily explained from a thermodynamic perspective. Apart from different electrochemical potentials at two sides, the electrochemical process also shows sharp entropy change. The reactions at both electrodes are shown below:

$$(Hot\ cathode)\ I_3^- + 2e^- = 3I^- \mid 3I^- + 2e^- = I_3^-\ (Cold\ Anode)$$

During the redox reaction, every single triiodide ion is converted from three iodide ions, which contributes to the sharp entropy change of the system. However, the thermoelectrochemical performance of I^-/I_3^- redox couple cannot at all be called outstanding compared with other electrochemical systems. To be specific, the I^-/I_3^-

system only has a Seebeck Coefficient of 0.53mV/K([27], Abraham, et al., 2013: 87-93.), which is much smaller than that of $Fe(CN)_3/Fe(CN)_6$. Despite its poor Seebeck Coefficient, the redox couple of I^-/I_3^- has been extensively investigated for its capability of stably converting heat into electricity in low-grade thermal gradient, and the potential of improvement in thermoelectrochemical performance with the help of chemicals inside the electrolyte. Due to the smaller molecular size of triiodide ion, inclusion reaction can contribute to thermoelectrochemical voltage, while it is not applicable to other redox couples of larger molecular sizes. It has been reported by Hongyao Zhou([27], Abraham, et al., 2013: 87-93.) that α-cyclodextrin (α-CD) can enhance the Seebeck Coefficient of I^-/I_3^- redox couple to a large extent by the inclusion reaction with triiodide ions at the cold anode of the system.

Since α-CD preferably reacts with I_3^-, which mainly exists at the cold side of the system, such reaction can be perfectly applied to thermoelectrochemical cell to improve the electrochemical potential. At the cold anode of the cell, triiodide ions will be trapped by the inclusion with α-CD([28], Tuza, et al., 2014: 2836-2843.), leading to a concentration decrease of triiodide ions. According to the Nernst Equation (1-2):

$$E_{therm} = E_{therm}^{\circ} - \frac{RT}{2F} ln \frac{\gamma_{I^-}^3 [I^-]^3}{\gamma_{I_3^-} [I_3^-]} \tag{1-2}$$

The inclusion reaction effectively decrease the concentration of triiodide ions inside the solution, thus enhance the total electrochemical potential of the system, leading to a higher Seebeck Coefficient. According to the experiment, the Seebeck Coefficient of the I^-/I_3^- system can be improved for 70% by employing α-CD for inclusion reaction, reaching a maximum level of 2.0mV/K.

Because of the hypotoxicity, stable chemical properties and low cost, the I^-/I_3^- redox couple has been introduced into many fundamental research of thermoelectrochemical cells. It has also been regarded as the candidate for

thermoelectrochemical cell with potential of scalable application. Moreover, Seebeck Coefficient of the I^-/I_3^- system can be maintained at a high level in low-grade thermal gradient, even near room temperature. Such feature makes it most suitable for heat harvesting during evaporation.

1.2.4 Methods to enhance the performance of thermoelectrochemical cells

Apart from choice of of redox couples, in previous research on the thermoelectrochemical cell, many strategies have been investigated by other groups to optimize the Seebeck Coefficient and thermal efficiency of the cell. Methods have been taken to improve the performance of thermoelectrochemical cell from the perspectives of mass transportation, electrode surface area, electrochemical reaction.

SyedWaqar has applied PVDF membrane in the experiment([29], Hasan, et al., 2016: 29328.) to limit mass transportation and attain a higher thermal gradient. PVDF membranes have been inserted at different positions of the thermoelectrochemical cell to limit water flux, which helps heat diffusion and undermines thermal gradient. The work reveals that by putting a PVDF membrane at the middle of thermoelectrochemical cell, the thermal gradient can be enlarged for 20℃, and maintained for a longer time. The sharper thermal gradient will, in return, enlarge the open-circuit voltage, according to Seebeck Effect.

Theodore has demonstrated that the electro-catalytic and surface area of electrode materials have great influence on thermoelectrochemical performance([30], Abraham, et al., 2014: 2527-32.). In Hyeongwook's work([31], Im, et al., 2016: 10600.), CNT aerogel sheets with porous structure decorated with catalytic platinum nanoparticles have been employed as electrode materials for current collecting. By removing of low

active carbonaceous impurities, the transfer of electron can be further enhanced. The aerogel sheet has been mechanically compressed to attain better conductivity and porosity, to collect current at a higher efficiency. This research, has improved the current level to a larger scale by decorating a porous electrode, thus improved the thermal efficiency of thermoelectrochemical cell.

Synergistic thermoelectrochemical redox couples have been employed by E. H. B. Anari([32], Anari, et al., 2016: 745-8.) to enhance both the Seebeck Coefficient and overall power efficiency. In the work, redox couples of ferrocenes and iodine have been applied in the same thermoelectrochemical environment. Charge-transfer complexes have been formed with ferrocenes and iodine, which effectively improves the electron-density of ferrocene. The improvement of electron density results in the highest Seebeck Coefficient of 1.67mV/K, which is higher than that of separate ferrocene or iodine redox couple system.

In our work, since both interfacial evaporation performance and thermoelectrochemical performance are important, we have focused more on optimizing the efficiency of our system from the perspective of evaporation surface. By achieving a shaper thermal gradient with a better evaporation surface using heat localization, thermoelectrochemical efficiency can be eventually improved.

1.3Thermoelectrochemical cell enabled by interfacial evaporation

Current researchers have been focusing on the investigation of thermoelectrochemical cells as a replacement of traditional solid state thermoelectric devices. Electrodes and electrolyte have been packaged into a single device, and placed in the environment with high thermal gradient to harvest the waste heat. Although thermoelectrochemical cells have slightly higher Seebeck Coefficient than traditional thermoelectric materials

with relatively lower cost, they may not be able to replace the solid state thermoelectric devices. A packaged thermoelectrochemical cell needs much larger space than thermoelectric membranes, A multiple-layered thermoelectric device, that takes the same space, can generate a much higher voltage. The biggest advantage of thermoelectrochemical cell is that it can harvest from low-grade thermal gradient with specific electrolyte, and that it can be applied to heat harvesting in liquid environments. By making use of the advantage, thermoelectrochemical cells can be applied for heat harvesting under specific circumstances, where traditional thermoelectric materials cannot be employed.

As mentioned above, interfacial evaporation for sea water desalination is one of the circumstances, where the capability of harvesting heat in low-grade thermal gradient and flexibility of thermoelectrochemical cells can be perfectly utilized. To combine interfacial evaporation and thermoelectrochemical cell, evaporation surface materials with outstanding performance must be selected to receive more energy from solar radiation and maintain heat localization. In the meantime, a suitable type of thermoelectrochemical system also needs to be selected for effective heat harvesting under the low-grade thermal gradient of interfacial evaporation system, without ruining the water desalination process. In addition, sea water desalination has been a large-scale application for both interfacial evaporation and thermoelectrochemical cell. The cost of evaporation surface materials and thermoelectrochemical electrolyte need to be limited for practical applications. In our experiment, rGO has been selected as the evaporation surface materials, due to remarkable intrinsic solar absorption, capability of pollutant removal and, most importantly, its lower cost than AuNP membrane as evaporation surface. The redox couple of I^-/I_3^- has been employed as thermoelectrochemical system, due to its outstanding performance in low-grade thermal gradient, lower cost than other types of electrolyte and, most importantly, its hypotoxicity, which assures that the additional electricity generation during interfacial evaporation will not affect the water purification.

Here, we exploit a multifunctional device that combines the electricity generation and water purification through interfacial evaporation by employing rGO membrane as evaporation surface materials and I^-/I_3^- redox couple as the basis of our electrolyte, which are both potentially low-cost and highly efficient for the desired applications. (**Fig. 1.**)

After review of other research on electrolyte based on I^-/I_3^-, KCl and α-CD have been added to the solution to increase the Seebeck Coefficient. Unlike other thermoelectrochemical cells packaged as a sealed thermoelectric device, our device is exposed to the open air and with strong thermal convection, which is avoided in the test of Seebeck Coefficient in other experiments. So both horizontal and vertical experimental systems have been made to test the approximate Seebeck Coefficient of our system, which can be a little lower than theoretical value due to thermal convection. Different types of evaporation materials, including graphite, paper-based rGO, graphite-based rGO, have been investigated for the better performance of interfacial evaporation and heat localization. To optimize the current as well as electrochemical efficiency, graphite foam was used to replace the platinum wire as better current collector. And the possibility of employing interfacial evaporation materials as electrode to maximize the temperature around the electrode has also been investigated. During the energy conversion process, the mass transportation is needed in order to maintain the electrochemical reaction, while it should be limited since such process can effectively undermine the thermal gradient. To reach the balance the two factors, thermoelectrochemical cells with different volume (height) of electrolyte have been compared for their maximum voltage and the capability of maintaining the voltage. Thermal insulators made of solid and porous silicone elastomer has later been introduced to our system for better heat localization to improve the evaporation efficiency as well as to attain a higher environmental temperature of cathode for higher voltage. By doing all of the experiments above, we have finally determined the

best system for our thermoelectrochemical cell enabled by interfacial evaporation. We also tested the evaporation rate, photothermal efficiency and thermoelectrochemical efficiency. The evaporation rates with and without thermoelectrochemical electricity generation have been compared to testify the influence of electricity generation upon interfacial evaporation and to see how much the energy conversion efficiency of the whole system has been improved by thermoelectrochemical cell. We have finally come up with a feasible plan for scalable application, with which, the solar energy of a specific area can be harvested by a higher efficiency for continuous electricity and steam output.

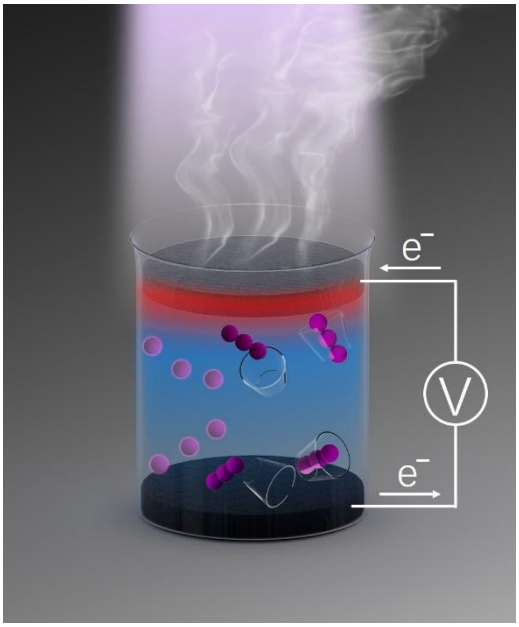

Fig. 1. Thermoelectrochemical cell based on I^-/I_3^- with KCl and α-CD, enabled by interfacial evaporation. Inclusion reaction between I_3^- and α-CD occurs at the cold side to further enhance the open-circuit voltage.

The importance of our work is not only to test the feasibility of evaporation-enabled thermoelectrochemical cell, which is flexible and has considerable Seebeck Coefficient. Moreover, by harvesting the waste heat during interfacial evaporation, the solar radiation can be conversed and utilized at an unprecedented high efficiency. Such combination brings us one of the possibility of solving the two biggest problems

of our current society and the inspiration of how to make better use of solar radiation.

Chapter 2 Experimental Methods

2.1 Synthesis of electrolyte solution

After making comparison of difference types of thermoelectrochemical electrolyte, we finally determine to adopt solution of I3-/I- redox couple as our electrolyte. α-cyclodextrin (α-CD) and KCl have also been added to the solution to induce a sharper concentration difference by inclusion reaction, as well as to improve the electronic conductivity of the whole system. The final formula of our electrolyte solution is as follows:

207.5mg KI, 1492mg KCl, 486.42mg α-CD and 63.4mg I2 in 100mL solution.

After trying to prepare the solution with different sequence of adding the chemicals, we found that KI and I2 should be put into the water first and dissolve with the aid of ultrasound. α-CD and KCl should be added next. This would help to distribute I- as uniform as possible, which can also reduce the time of obtaining a stable solution.

2.2 Test of Seebeck Coefficient in our system

Although the feasibility and Seebeck Coefficient of the electrochemical cell of I-/I3- has already been mentioned and testified in previous research, test of our

electrochemical cell is still needed since our thermoelectrochemical cell works in a beaker rather than a U-tube, which is used by most of other researchers. In the U-tube, convection inside the solution has been limited to the minimum level by restricting the current flow, thus it can induce a higher concentration difference than our system, despite of the same thermal gradient.

So, we have made a horizontal glass box to test the Seebeck Coefficient of our electrolyte with external heat source and cold source. We finally came up with reliable Seebeck Coefficient, which can be applied to our evaporation system and also matches well with the data mentioned in the reference with only minor difference due to thermal convection.

2.3 Synthesis of GO solution and hydrothermal method to reduce GO into rGO

In our experiments, rGO has been chosen as the evaporation surface material duet to its wide absorption spectrum of solar radiation and function of heat localization. In our work, the rGO is initially paper-based, which is the most reliable method, testified by many previous studies. The carrier of rGO has then been changed into graphite foam, which can serve as both solar receiver and electrode material in the meantime. More importantly, graphite foam also has a better performance of heat localization, due to its porosity, which can help limit the heat diffusion from surface to the system. The rGO membrane has been synthesized through two different methods: 1. Synthesize rGO separately, and drop it on the cut airlaid paper manually. 2. Synthesize GO first, and apply the hydrothermal method to reduce the GO into rGO and assemble it on the surface of carrier in a reactor. We succeeded in both methods of synthesis, and the second method was adopted, which can distribute rGO onto the paper more uniformly.

The GO solution in our work was synthesized by the following procedures:

We mixed 0.5g graphite powder and 0.5g NaNO3 with magnetic stirring, and then immersed in ice cold water to let it cool down. Then 40mL concentrated sulfuric acid was added into the mixture. Three grams of $KMnO_4$ was then also added into the flask and the solution was kept stirring until it becomes uniform. Then the solution was stirred in 40℃ water bath for 1h and 30 mL deionized water was added into the flask. After reacting for half an hour, 100 mL water has been added into the solution. At last 3 mL H_2O_2 has been added into the solution at a rate of 12 mL/h under sufficient stirring. Finally, the solution has been centrifuged at the speed of 1000 r/min and 8000 r/min separately to get rid of the impurities.

After drying the final solution mentioned above, we can obtain the GO powder. Then we applied hydrothermal method to assemble rGO onto the surface of airlaid paper and graphite foam, which is described as the following:

GO powder was dispersed into deionized water to reach the concentration of 1 mg/mL, further disperse the GO was done with the help of ultrasound. After that we used a pipette to drop 1 mL solution onto a paper, and then dried the paper in the oven. This procedure has been repeated for several times until the GO was uniformly coated in the paper. For an air-laid paper with size of 15.2 cm^2, 6mL of GO solution has been used. The dried paper with GO was placed into the sealed reactor and immersed in the mixture of 10 mL ethanol and 20 mL deionized water. The reaction was lasted for 3h in the oven of 120℃, and then the paper was taken out and dried.

Same hydrothermal method of reduction has been applied to graphite foam. However, 20mL of GO solution has been used for a graphite foam with same projection area as the air-laid paper, due to the relatively larger thickness of graphite foam.

2.4 Characterization of evaporation surface

In order to find out the most suitable materials as evaporation surface material, characterizations of evaporation surface materials including physical properties and morphologies need to be done to make the comparisons. Three evaporation surface materials candidates, including paper-based rGO, graphite foam, and graphite-based rGO have been tested to get their capabilities of intrinsic solar absorption by testing their UV-Visible Absorption Spectra. SEM (Sirion 200) with magnifications of 1000X and 5000X have also been made to characterize the morphology of the samples, and to check the distribution of rGO on graphite foam and airlaid paper. With the above two methods of characterization, it can be predicted which type of material has better evaporation performance, thus this can help us decide the most suitable material to use for our evaporation enabled thermoelectrochemical cell system.

2.5 Synthesis of thermal insulator of silicone elastomer

Inspired by research of interfacial evaporation, thermal insulator has also been employed in our system, since the heat localization improved by insulator is the key factor to both evaporation efficiency and electricity generation. The thermal insulator, in our system, must be a nonconductor, or its contact with our graphite electrode may affect the process of electricity generation. Among all the thermal insulator candidates, insulator made of silicone elastomer has finally been picked based on its outstanding ability of thermal insulation due to the porous nature, and simple synthesis process.

In our work, silicone elastomer (Sylgard 184, part A) and foaming agent (Sylgard 184, part B) have been mixed in the ratio of 1:1 to synthesize the porous thermal insulator. To maintain the insulator with appropriate buoyant force in electrolyte, which can support the electrode material but still keep it immersed in the solution, insulators

with different amount of silicone elastomer have been used. The most suitable thermal insulator is made by adding 5g of silicone precursor and 5g of foaming agent into the watch-glass, stirring sufficiently until the uniform mixing of the two parts be achieved, and solidify the mixture at room temperature. Then PDMS is made by mixing silicone elastomer (Sylgard 186, part A) and curing agent (Sylgard 186, part B) in the ratio of 5:1, and dried in the vacuum drier to get rid of bubbles inside. The solidified silicone elastomer was then dipped into the liquid PDMS and dried in the oven to seal the surface of insulator, which is to prevent water from coming into the insulator and undermine thermal insulation.

2.6 Test of evaporation efficiency

In our work, solar radiation of 400mW/cm^2 (4 times of sunlight on earth) has been applied to shorten the experiment time, as well as to simulate the concentrated sunlight used in water desalination in practice. The light source (GHX-Xe-300) runs at the voltage of 220V and current of 19A. The intensity of solar radiation has been testified by the optical power meter(PM100D) for accuracy. As mentioned in the introduction part, evaporation efficiency is calculated based on the evaporations rate at room temperature and under solar radiation. The result of true efficiency stands for the percentage of whole solar radiation, which has been used to transfer water into steam, and heat up the steam. In our work, evaporation efficiency of paper-based rGO, original graphite foam, and graphite-based rGO have been tested to compare their capability of photothermal conversion. Evaporation rates of the same system with and without electricity output has also been tested and compared to get the information about the influence of electricity generation on the evaporation performance.

2.7 Test of thermoelectrochemical performance

To select the most suitable match of evaporation surface, electrode materials etc., different systems have been tested using a data collector (34972A) for their open-circuit voltage (recorded for 5mins in room temperature and 30mins under 400mW/cm^2 solar radiation), short-circuit current (recorded for 30mins under 400mw/cm^2 solar radiation after being heated up with open circuit for 30mins) to compare their maximum voltage, maintenance of voltage, maximum current, maintenance of current. For the selected most suitable system, maximum output power has also been tested, by measuring the voltage of different resistances connected to the thermoelectrochemical cell. By calculating the power of external resistance using (2-1):

$$P = \frac{U^2}{R} \tag{2-1}$$

The external resistance, which has the maximum output power, has been employed to test evaporation rates difference between the process with mere evaporation and maximum electricity output.

2.8 Test of cycle performance

In our work, a concept of evaporation and electricity generation cycle has been raised as a method of scalable application. In the application, the thermoelectrochemical cell is firstly exposed to solar radiation of 400mW/cm^2 for 15mins, and then covered up in room temperature for 40mins. It is then cooled down in room temperature for 20mins and added with deionized water to make up the mass loss. In the repeated experiment, we have tested the maximum electricity output power and evaporate rates during the first two steps, to calculate the sum of total amount of electricity and evaporated water induced by the solar radiation of 15mins. In this case, we can calculate the total electricity output power and compare it with the electricity output at steady state

evaporation. By this comparison, we can testify to what extent that, our cycle plan has increased the energy harvested from solar radiation.

Chapter 3 Results and Discussion

3.1 Horizontal test of Seebeck Coefficient with external heat and cold sources

We have manually made a horizontal glass box, which is assembled by six glass slides of the same thickness, and can applied in the test of Seebeck Coefficient with inner convection. Graphite rods, as electrode materials, have been put at both sides of the box (cathode to the cold side and anode to the hot side) with thermocouples to test the environmental temperature of electrodes. External heat source and cold source have also been put at both sides outside the glass box, providing different external thermal gradient by using different input voltage. In our work, the input voltage of heat source and cold source have been controlled to be 12V, to provide heat source and cold source of relatively the same power.

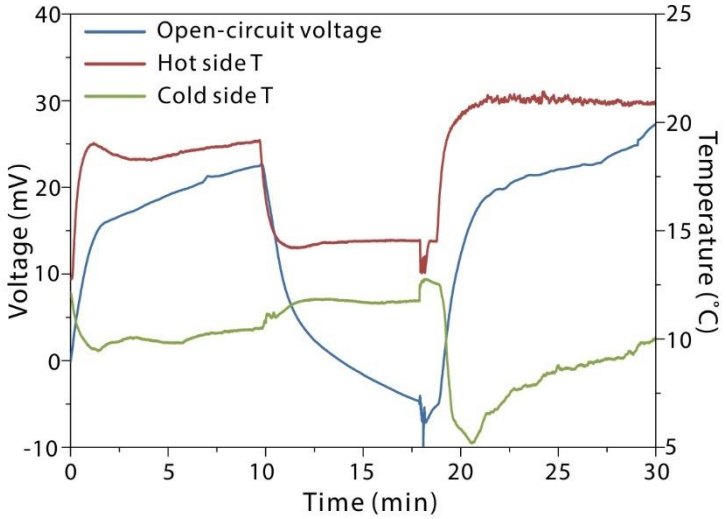

Fig. 2. the Seebeck Coefficient tested with external thermal gradient is approximately 1.45mV/K, which is smaller than 2.0mV/K due to inner convection.

In our experiment, the heat source and cold source have been turned on at the beginning, and remained for 10 minutes (**Fig. 2.**). With the temperature increase and drop at hot side and cold side respectively, the voltage increases in the positive direction from zero immediately. After the first 10mins, external heat and cold have been turned off for 10 minutes for the temperature at both sides to return back, which also induces the drop of open-circuit voltage. At the third step, the heat and cold source at both sides have been turned on for another 10 minutes to record the change of open-circuit voltage.

It should be stated that, in this experiment, we have put cathode at the cold side by accident, which induces the increase of voltage in negative direction rather than predicted positive direction. From the data collected in this experiment, we can firmly state that the Seebeck Coefficient in our system is about 1.45mV/K, which is smaller than 2.0mV/K as reported in Hongyao Zhou's research, due to the strong inner convection in our system. With the strong inner convection, the concentration difference at both sides may not be sharp enough as reported, despite the same solution components.

In the meantime, since KCl is also an important component of our system, though never reported before, we have to testify whether Seebeck Coefficient exists in KCl solution or not. After carrying out the experiment with graphite electrodes, no Seebeck effect of KCl solution have been detected.

3.2 Vertical test of Seebeck Coefficient with solar radiation

After testing Seebeck Coefficient in the glass box with external thermal gradient, we confirm the feasibility of our system with considerable inner convection. However, whether our thermoelectrochemical cell can be enabled by interfacial evaporation remains to be seen, since in our system, gravity is also going to play an important role in both mass transportation and ion diffusion, and that the temperature difference induced by interfacial evaporation remains unknown.

To combine interfacial evaporation and thermoelectrochemical cell to test the feasibility, a special beaker has been designed, which has two openings at one side separately at the top and bottom for inserting of electrodes and thermocouples. The paper-based rGO has been chosen as the evaporation surface materials, since its performance of solar absorption and heat localization has been testified by many former research, and it will not have any side effect on electricity generation. In the meantime, Platinum wire has been chosen as electrode materials. After ultrasound wash with hydrochloric acid, acetone and deionized water, platinum wire is guaranteed not to have surface absorption and reaction with electrolyte, which may affect the detected voltage.

After inserting the Pt electrodes and thermocouples into the beaker, we later fill the beaker with our electrolyte solution and carry out the experiment under solar

evaporation of 400mW/cm^2, at the room temperature of 18.9℃ and relative humidity of 46.3%. The evaporation rate of the electrolyte solution in a 100 mL beaker with paper-based rGO surface is 1.343867 mg/s under the solar radiation, while evaporation rate of the solution with rGO in room temperature without the light is 0.054222 mg/s. Thus, the irradiation induced evaporation rate is 1.3289645 mg/s. With the evaporation surface of 15.2cm^2, the true efficiency of photothermal conversion was calculated to be 53.307%. The result proved the paper-based rGO surface is a reliable evaporation surface for photothermal conversion as reported.

Thermal gradient induced by solar absorption and heat localization of rGO film has also been tested by both record of thermocouples and IR images. According to the IR images below (**Fig. 3. A&B**), a temperature difference of more than 20℃ between the top and bottom can be formed, during the interfacial evaporation of paper-based rGO film. By heating up the water mostly at the surface and vaporize the water without heating up the bulk liquid, the evaporation surface creates and maintains the thermal gradient, which can fulfill the requirement of thermoelectrochemical cells.

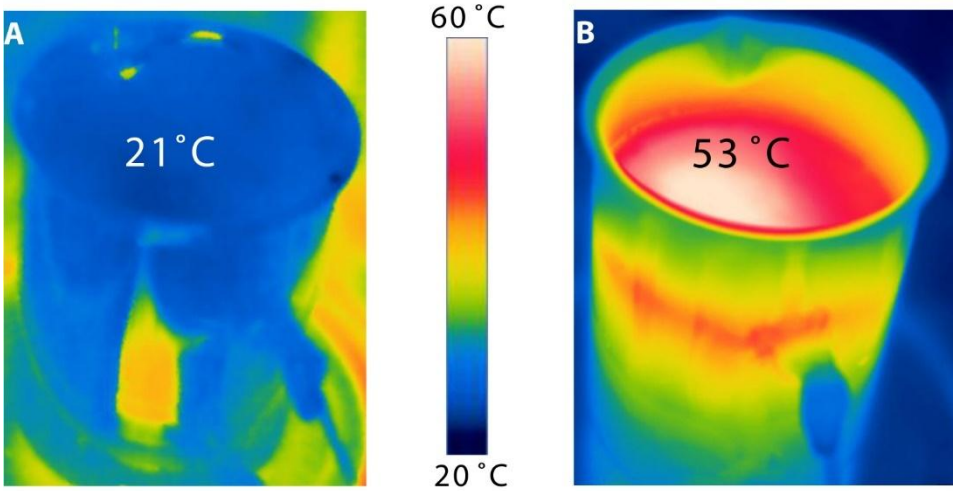

Fig. 3. IR images of the electrolyte solution at room temperaure and under the solar radiation of 400mW/cm^2. **A.** the surface of paper-based rGO is 21℃ in room temperature. **B.** With the solar absorber of paper-based rGO, the temperature of evaporation surface raised to 53℃ with solar radiation, while the temperature at the

bottom was kept at 33℃.

In addition, according to the data collected by thermocouples, the top and bottom temperature will finally stay at a level of 53℃ and 33℃ separately, maintaining a temperature difference of 20℃.

Data of thermal gradient and voltage have then been combined to test how the Seebeck Effect works in our interfacial evaporation system. At the beginning of the experiment, the voltage and the temperature difference between top and bottom increases dramatically, and reaches the highest level in a short time. The relationship between the voltage and temperature difference matches well with the Seebeck Coefficient tested in the glass box. The reduction of I_3^- at the top and the oxidation of I^- at the bottom contribute to the voltage coherently. The voltage also becomes higher due to the inclusion reaction between I_3^- and α-CD. As the experiment continues further, the thermal gradient induces not only voltage but also convection inside the solution. Such convection led to the heat up of the whole solution. As the temperature difference remains, the voltage of our thermoelectrochemical cell becomes stable after ~10 mins of solar irradiation. At the steady state, the voltage and both the temperatures at the top (53℃) and bottom (33℃) almost remain constant (**Fig. 4A**).

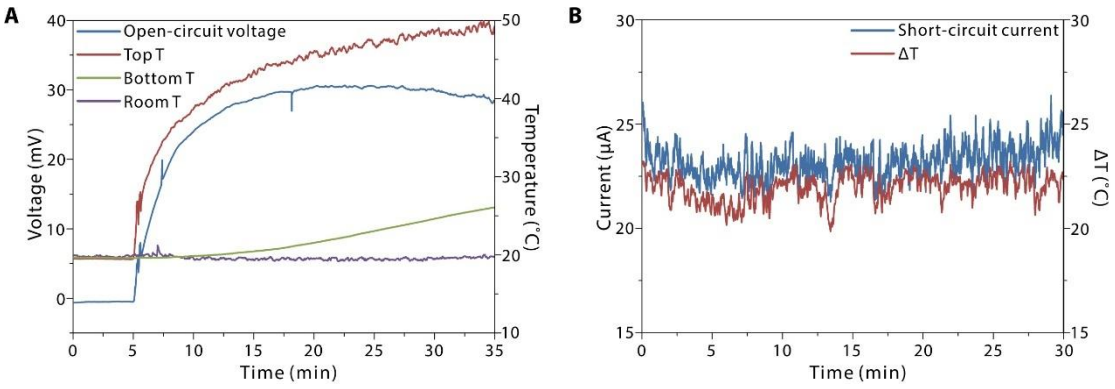

Fig. 4. A. The voltage change during the initial stage of solar radiation. The open-circuit voltage of our system increases immediately, when the solar radiation

tarts to work and the thermal gradient starts to form. It however, experiences a slight drop, as the temperature at the bottom increases, despite the constant temperature difference. **B.** The current at the steady state. The current of the system almost remains the same in the steady state of evaporation, since the thermal gradient is now maintained.

By measuring the current of the thermoelectrochemical cell, we found that the current also stays the same at the steady state along with thermal gradient (**Fig. 4B**). However, sustainable though, the current system with paper-based rGO as evaporation surface and Pt wires as electrodes exhibit relatively poor electrochemical performance. Although the voltage matches perfectly with existing thermal gradient according to Seebeck Coefficient, strategies should be investigated to enlarge and maintain the thermal gradient, in order to attain a higher voltage. Apart from, the current value right now is only 24μA at steady state is also far from satisfactory for scalable applications, methods to optimize the current and electrochemical efficiency is badly needed.

After testing the feasibility and sustainability of thermoelectrochemical cells enabled by bio-inspired interfacial evaporation, later experiments have been focusing on strategies to optimize the evaporation performance and thermoelectrochemical performance. Different systems have been proposed to enlarge the voltage and current, while also trying to attain maximum evaporation rate.

3.3 Thermoelectrochemical cell with bifunctional graphite foam act as both electrode and evaporative surface

To improve the current and efficiency of the cell, electrodes with larger surface area are required, since larger surface area means the redox reaction can happen at a higher

rate and consequently lead to higher current level of the cell. In this case, electrode materials, which will not react with our electrolyte, and in the meantime, is porous and cheap enough should be investigated as satisfactory candidate for electrode materials.

In the meantime, methods to increase the environmental temperature of the upper electrode are also guaranteed to increase the voltage of thermoelectrochemical cell due to Seebeck Effect. There is no doubt, that the evaporation surface is the part with highest temperature in our system. If we can use evaporation surface as electrode at the top of the system, the temperature of the top electrode can be increased to a large scale, thus sharply increase the voltage of our thermoelectrochemical cell in evaporation.

The graphite foam, with its porous nature and outstanding conductivity, is originally employed as a type of ideal electrode material. In the meantime, due to the wide intrinsic absorption spectrum of graphite foam, it is believed to perform well in interfacial evaporation. What's more, due to porous structure of graphite foam, it also has the function of thermal insulation, since some of the air can be locked inside the unconnected pores inside the graphite, restricting the heat from diffusing to the bulk volume of water. The thermal insulation can contribute to heat localization, which can help form a higher environmental temperature for the top electrode, thus enlarger the voltage and evaporation rate of our system.

In this case, we have adopted graphite foam as the first bifunctional material as both electrode and evaporative surface in the meantime. The graphite foam has also been cut into the shape with a top surface area of 15.2cm^2. It is washed by deionized water, dried, and put into the plasma cleaner (PDC-32G) for better hydrophilicity. Then the graphite foam is pierced by the Pt wire, and serves as electrode material together with Pt wire. The electrode at the bottom has also been replaced by graphite foam with Pt

wire, to assure a better performance of current collecting (**Fig. 5A**).

Due to the possible touch between the thermocouple and graphite foam electrode, which has been tested to be able to affect the detected value of voltage, thermocouples in the system has been removed from now on. The level of heat localization and approximate value of thermal gradient has now been tested via IR images (**Fig. 5B**). In the experiment of employing graphite foam as both electrode and evaporation surface, the thermoelectrochemical cell has also been exposed to the stable solar radiation of 400mW/cm^2, and the evaporation rates were tested at room temperature at the steady state of light-induced evaporation, at the room temperature of 24.3℃ and relative humidity of 46.7%.

The evaporation rate of the electrolyte solution in a 100 mL beaker with graphite foam surface is 1.39012mg/s under the solar radiation, while evaporation rate of the solution with graphite foam in room temperature without the light is 0.0546205mg/s. Thus, the irradiation induced evaporation rate is 1.34392mg/s. With the evaporation surface of 15.2cm^2, the true efficiency of photothermal conversion was calculated to be 55.842%. The result proves that the graphite foam as evaporation surface has better performance than paper-based rGO, because of its better intrinsic solar absorption of slight thermal insulation. The information collected from IR image matches perfectly with the result of evaporation rate calculation. The graphite foam has increased the surface temperature from 53℃ to about 60℃, which implies a better heat localization and higher evaporation rate. Such increase at the top surface is believed to enlarge the thermal gradient and the environmental temperature of the top electrode, especially when the evaporation surface has been directly applied as electrode.

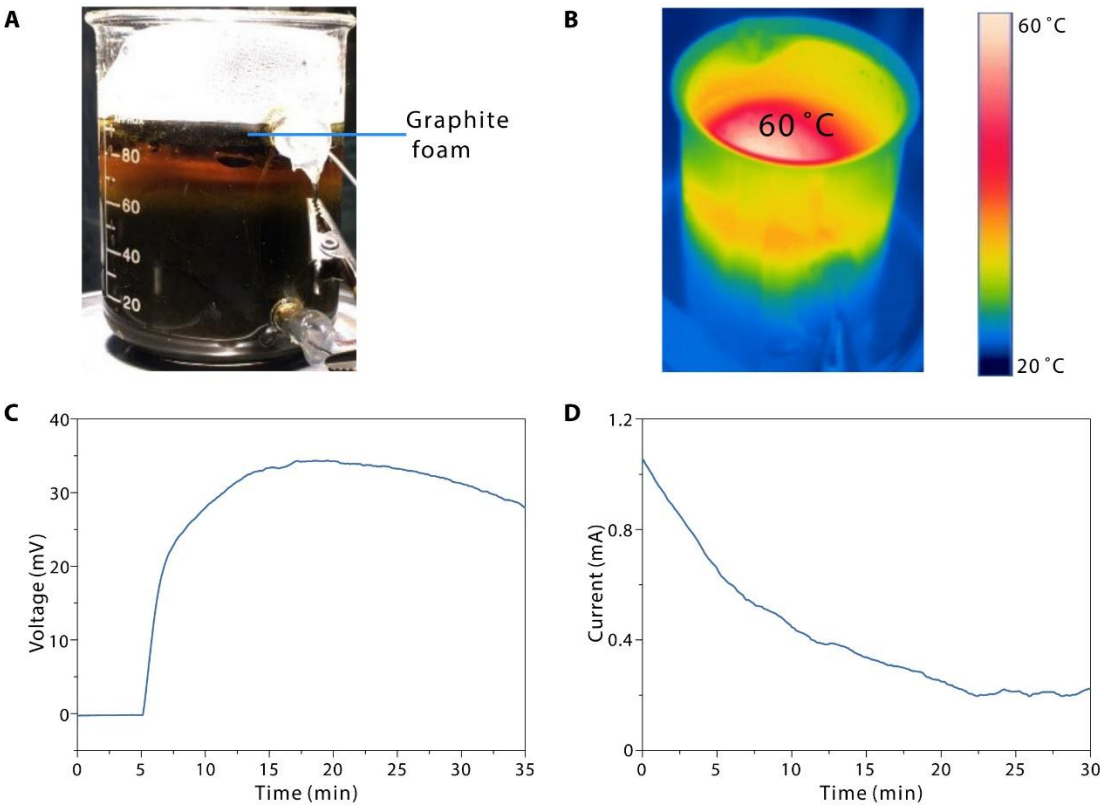

Fig. 5. A. The experimental equipment under solar radiation with graphite foam bifunctional as both evaporation surface and electrode. **B.** With a better solar absorption and slight thermal insulation, the temperature of evaporation surface has been increased to 60℃, which is greatly higher than that of paper-based rGO. **C.** Due to sharper thermal gradient, formed with the help of graphite foam as evaporation surface, the open-circuit voltage has been increased to 35mV. **D.** While the voltage has been increased for 5mV, the current has been increased to a maximum level of more than 1mA, then drops and stays at 200μA in steady state, as the thermal gradient decreases at the beginning and then remains the same in steady state.

As predicted by the information given by IR image, our system with bifunctional graphite foam as evaporation surface and electrode has increased the maximum voltage from 30mV to 35mV due to the higher temperature at evaporation surface (**Fig. 5C**). The voltage has also been effectively maintained due to the slight thermal insulation of graphite foam. While voltage has been slightly enhanced due to higher environmental temperature of upper electrode, the maximum current has been

dramatically increased to more than 1mA (**Fig. 5D**). The current at steady state still remains 200μA, which is about 10 times larger than that of Pt wire electrode, due to the larger surface area.

However, the current at steady state cannot be simply enlarged by the ratio of surface area between graphite foam and Pt wire. Since the current of our system is not merely restricted by how fast the electrochemical reaction at happen near the electrode, but also the of diffusion rate of components, which maintain the concentration of reactants near the electrode. Current at steady state can only be further enhanced, when the mass transportation and diffusion of components has been increased somehow. While mass transportation and diffusion of components are beneficial to electrochemical reaction rate, thus can increase the current, such two factors are the least desirable factors in interfacial evaporation and maintaining the thermal gradient. There is no doubt that higher speed of mass transportation and diffusion of components will induce higher rate of thermal diffusion from the top to bottom, which can eventually undermine the thermal graphite and voltage of the system.

To balance the such two contradicting roles of mass transportation and components diffusion, experiments have been carried out in systems with different volume of electrolyte solution to test most suitable amount of solution for the maximum thermoelectrochemical properties. The smaller volume (height) of solution, the shorter path for the mass transportation and components to go through, which means better mass transportation and better thermal diffusion. In all the experiments, graphite foam has been employed as evaporation surface and electrode materials to optimize the voltage and current.

3.4 Test of thermoelectrochemical cells with different amount of electrolyte

Although we have replaced the electrode material with graphite foam, which has much larger surface area and the current increases to a large extent, the current can hardly be enhanced further, limited by reactant concentration rather than reaction rate. The stable current means the reaction must happen at a constant rate continuously, which requires the component concentration to be maintained by mass transportation. Mass transportation originally exists in the system, especially when there is a thermal gradient. However, due to the long path for components to travel from the bottom to the top, the mass transportation inside the solution right now is not enough to maintain a current. In this case, we come up with the plan to carry out the experiments with less amount of electrolyte solution, in which the cycle of mass transportation is shorter and a higher diffusion rate of components can be expected.

In our work, we have set up the systems with electrolyte solution of 40mL, 60mL, 80mL, and the original amount of 100mL to make comparisons. All the systems have been put in room temperature for 5mins at the beginning, and then exposed to solar radiation of 400mW/cm^2 for 30mins to test voltage. Current data has been collected during the 30mins right after the voltage test finishes. The results are shown below (**Fig. 6.**)

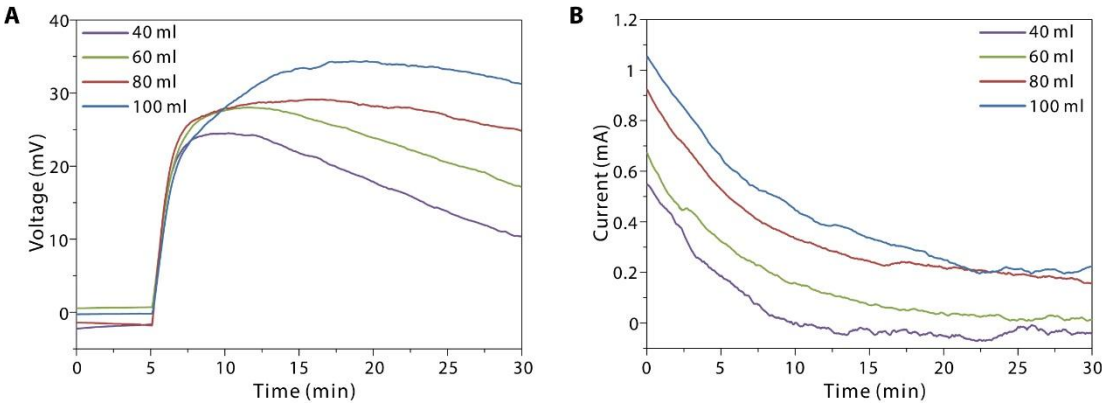

Fig. 6. A. The open-circuit voltage of different systems with electrolyte solution amount of 40mL, 60mL, 80mL, 100mL. The maximum voltage and the sustainability have been both improved since the thermal gradient can be enlarged and remained with larger volume of solution. **B.** The current of the systems is also better in the systems with larger amount of electrolyte solution.

As shown in the (**Fig. 6. A&B**) above, in the group of 40mL, the maximum voltage only reaches about 25mV under solar radiation. And due to the faster mass transportation and shorter path for thermal diffusion, the thermal gradient between the top and bottom can hardly be maintained, which causes the temperature increase at the bottom, and dramatic voltage decline along the experimental process. And during the current test, the whole bulk electrolyte has been further heated up due to effective thermal diffusion, till the temperature difference between the top and bottom can even be ignored. That's why the current data falls sharply during the test, and finally reaches the value of about zero and even negative. At the final stage of the current test, because of the approximately same temperature at top and bottom, the Seebeck Effect is no longer dominant in the system. In the meantime, due to the role of gravity inside the system, reactant concentration at the bottom remains larger than the top. The weak current in the negative current is therefore formed by the concentration difference. And all the data shown in the figure exhibits the same tendency that with the increasing amount of electrolyte solution, the thermal gradient as well as the voltage can be better maintained. The maximum temperature also increases, since based on the slower thermal diffusion, a larger temperature difference between the top and

bottom can, therefore, be created. And according to the data of current, decrease of current have been detected in all groups because of the decrease of reactant concentration. However, the groups with larger volume of electrolyte solution exhibits a larger maximum current and stable current, since the voltage of the 80mL and 100mL groups can be better maintained. The group of the original amount of 100mL electrolyte solution, shows the best thermoelectrochemical performance during the test, due to its capability of maintaining the thermal gradient, and should be therefore be employed as the most suitable set up.

Although the decrease in electrolyte amount can effectively increase rate of mass transportation, mass transportation, in the meantime, also plays a contradicting role to undermine the thermal gradient, which will in return decrease the voltage generated by Seebeck Effect, and decrease the current. Such heating up of the whole volume of solution is also undesirable to improve the efficiency of interfacial evaporation. In conclusion, the thermal gradient seems to be prior to concentration diffusion to improve the total efficiency of the system. In this case, further methods to enlarge and maintain the thermal gradient need to be investigated to optimize the performance and efficiency of our system.

3.5 Characterization of different evaporation materials

As mentioned above, enlarging the thermal gradient of the system, is the most reliable method to improve the voltage and evaporation rate. Heat localization, the key factor to both thermoelectrochemical cell and interfacial evaporation, can be improved by gathering more heat from solar radiation by intrinsic absorption or by preventing the heat from dissipating to the environment. We herein, firstly, investigate the strategies for further enhance the intrinsic solar absorption of evaporation surface. So far, we have employed paper-based rGO and graphite foam as evaporation surface.

Paper-rGO works perfectly as evaporation surface, since rGO on the air-laid paper has a wide absorption spectrum of solar radiation. Graphite foam, due to its original black color, also has a wide absorption spectrum. However, the absorption of rGO may not be overlapped by that of graphite foam completely. That is to say, rGO can further enhance the evaporation performance, if it can be assembled on the surface of graphite foam.

We therefore synthesized the graphite-based rGO, by similar hydrothermal method, as evaporation surface and employ it as a candidate for evaporation surface material. To testify whether graphite-based rGO has a better performance than paper-based rGO and original graphite foam, characterizations of three types of materials should be done to compare their absorption spectrum and morphology. SEM of graphite-based rGO is also used to check whether our method of reducing GO on the surface of graphite foam has been successful or not. The results of UV-Visible Absorption Spectrum are shown below (**Fig. 7.**).

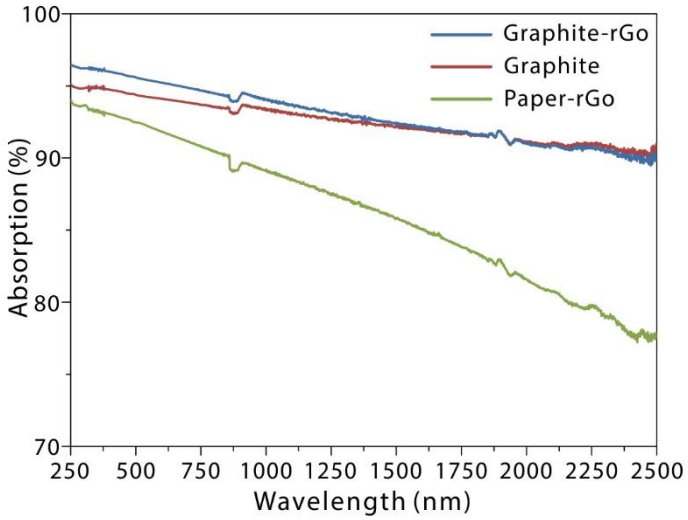

Fig. 7. UV-Visible Absorption spectra of paper-rGO, graphite foam and graphite-rGO. Both the solar absorption performances of graphite foam and graphite-rGO are better than that of paper-rGO. The rGO assembled on the surface of graphite foam has effectively enhanced solar absorption, especially in the short wavelength regime.

During the test of absorption spectrum, we have collected the data of transmission coefficient and reflection coefficient of three types of materials, and calculated the absorption percentage by subtracting them from 100%. The outstanding performance of solar absorption of three types of materials are revealed by the results. In the meantime, paper-rGO has the poorest absorption performance among three types of materials. And the rGO on the surface of graphite foam does slightly enhance the absorption performance of graphite foam, especially under the radiation of short wavelength.

SEM images are shown below to compare the morphologies of three evaporation materials. (**Fig. 8.**) According to the SEM results, rGO has been formed, and therefore, wrapped on the surface of the paper fibers, which affords the wide absorption spectrum of paper-based rGO. While the surface of graphite foam is relatively smooth, rGO has also been wrapped at the surface of graphite-rGO, which means our method of synthesizing rGO on the surface of graphite foam has been successful. Such morphology difference can also help illustrate why graphite-based rGO has better absorption performance than the original graphite foam as shown in the UV-Visible absorption spectrum.

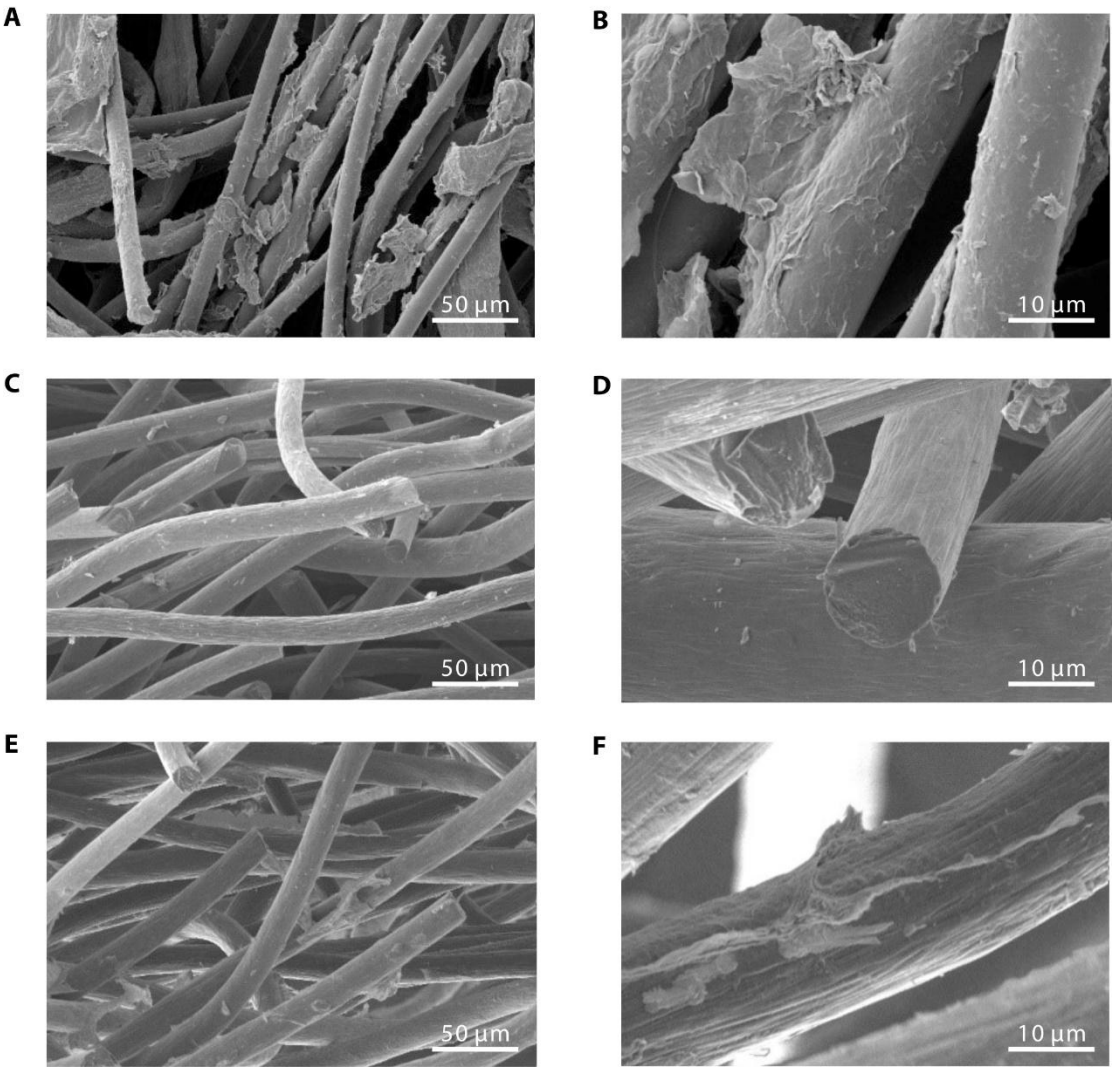

Fig. 8. SEM images of paper-based rGO, graphite foam and graphite-based rGO. **A.** paper-based rGO at 1000X. **B.** paper-based rGO at 5000X. **C.** graphite foam at 1000X. **D.** graphite foam at 5000X. **E.** graphite-based rGO at 1000X. **F.** graphite-based rGO at 5000X. The SEM images of graphite-based rGO shows that rGO has been successfully assembled on the surface of graphite foam.

So far, graphite-based rGO exhibits the best performance of solar absorption, thus is believed to bring about better heat localization and thermal gradient. Due to the perfect electric conductivity of graphite-based rGO, it can also be employed as electrode material in the meantime to maximize the environmental temperature of electrode. Therefore, it has been later employed as both evaporation surface and electrode materials to make comparison with former systems.

3.6 Thermoelectrochemical cell with graphite-based rGO as evaporation surface and electrode

Based on the results of characterizations of three types of materials, graphite-rGO has been selected as potential evaporation surface for its better performance of solar absorption. In our work, graphite foam has then been replaced by graphite-based rGO to carry out the experiment. In the experiment, the thermoelectrochemical cell is also put under the solar radiation of 400mw/cm^2, and tested the voltage, current and evaporation rate for the comparison of thermoelectrochemical performance and evaporation efficiency. This experiment is carried out at the room temperature of 22.5℃ and relative humidity of 41%.

The evaporation rate of the electrolyte solution in a 100 mL beaker with graphite-based rGO surface is 1.41065mg/s under the solar radiation, while evaporation rate of the solution with graphite-based rGO in room temperature without the light is 0.051367mg/s. Thus, the irradiation induced evaporation rate is 1.359283mg/s. With the evaporation surface of 15.2cm^2, the true efficiency of photothermal conversion was calculated to be 58.425%. It is no hard to figure out from the results, although the evaporation rate of our system has not been increased much with the application of graphite-based rGO as evaporation surface, by increasing the surface temperature, the true efficiency of our system has still been raised to a large extent.

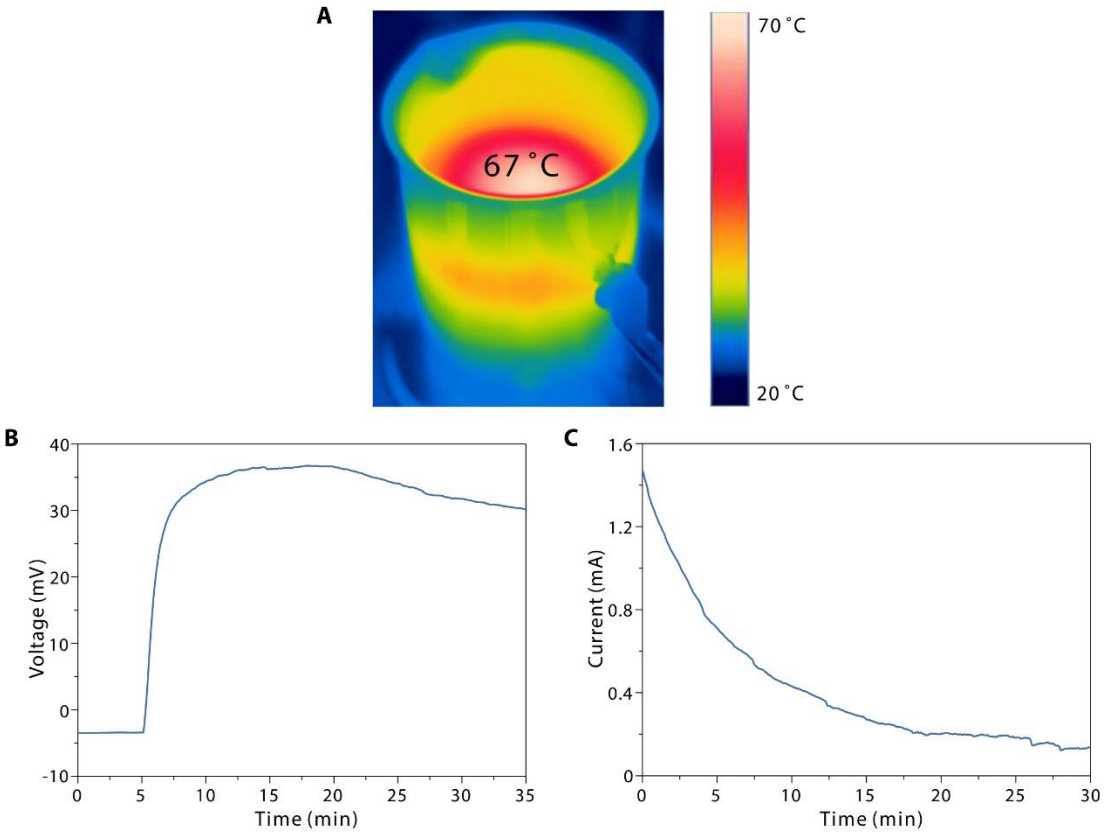

Fig. 9. A. IR image of thermoelectrochemical cell with graphite-based rGO under solar radiation of 400mW/cm^2, the temperature of evaporation surface has been increased from 60℃ to 67℃ by assembling rGO on graphite foam. **B.** Voltage data of thermoelectrochemical cell with graphite-based rGO. By forming a shaper thermal gradient with the help of rGO, the voltage has been further enlarged. **C.** Current data of thermoelectrochemical cell with graphite-based rGO. The current has been increased to a maximum level of more than 1.4mA, and gradually falls back due to concentration limit.

The better performance of solar absorption of graphite-based rGO is embodied as a higher surface temperature, detected by the IR camera. With the enhancement of rGO, the surface temperature of electrode has been increased from 60℃ to a maximum of 67℃ (**Fig. 9A**). Such increase in surface temperature has, consequently, enlarged the temperature different between the top and bottom, thus increase the voltage induced

by Seebeck Effect. The total voltage of the system has increased to a maximum of 37mV, and is also maintained at consider level during the 30 mins of solar radiation (**Fig. 9B**). The increase of voltage also leads to an increase of maximum current. The current, however, falls down eventually to the level of steady state due to the reach of the balance of reactant concentration (**Fig. 9C**).

After trying to optimize the heat localization by replacing the evaporation surface, and achieving a satisfactory result, strategy of thermal insulation should also be applied to improve the efficiency of thermoelectrochemical cell and interfacial evaporation. Many researchers' work on the function of thermal insulator on interfacial evaporation has proved its potential of enhancing the efficiency of our system. For this reason, we have then introduced a type of easy-synthesized thermal insulator to our system.

3.7 Thermoelectrochemical cell with thermal insulator made of PDMS

Thermal insulator, due to its porous nature, has very poor heat conductivity, and is, therefore, capable of enhancing heat localization. In our experiment, thermal insulator, made of porous silicone elastomer and sealed by polydimethylsiloxane, has been introduced to our system to form a higher temperature at the evaporation surface and electrode.

The synthesis process of thermal insulator has been explained in the experimental method. The thermal insulator made of PDMS has been put under graphite-based rGO electrode to prevent the thermal diffusion from the electrode into solution. The size of thermal insulator has been designed, to support the graphite foam electrode with buoyant force, but still assure that the graphite foam be immersed in the solution.

In our experiment, the system with thermal insulator under the graphite foam is shown below (**Fig. 10A**). IR images of the system under the solar radiation of 400mW/cm^2 have also been taken (**Fig. 10B**), to investigate the heat localization. Evaporation rates have also been recorded to calculate the true efficiency during evaporation at the room temperature of 22.7℃ and relative humidity of 42%.

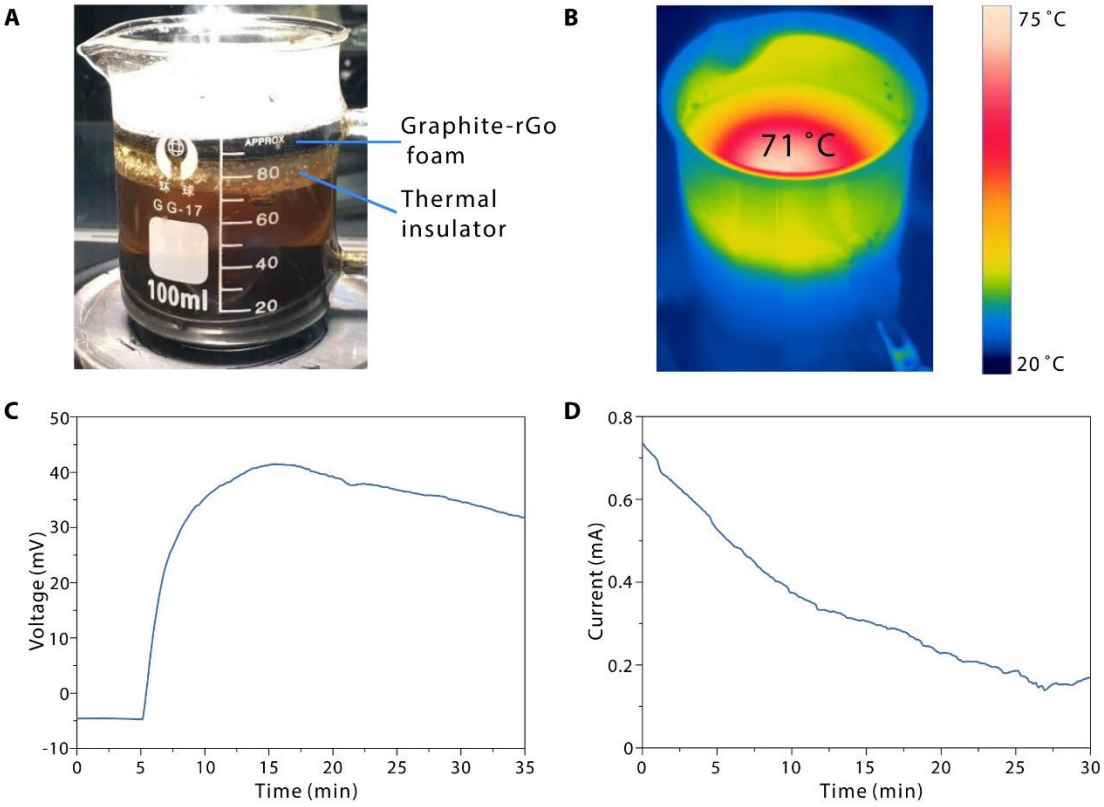

Fig. 10. A. The equipment of system with PDMS insulator under the graphite-based rGO. **B.** The IR image of the thermoelectrochemical cell under solar radiation of 400mW/cm^2. With the help of thermal insulator, the surface temperature has been increased to 71℃. **C.** The open-circuit voltage of the cell. With better heat localization achieved by thermal insulation, the maximum voltage has reached an unprecedented level of more than 41mV. **D.** Despite higher voltage, the current of the thermoelectrochemical cell becomes smaller, since the PDMS insulator limits ion transportation, but stays at a high level at steady state due to sharp thermal gradient.

The evaporation rate of the electrolyte solution in a 100mL beaker with

graphite-based rGO surface and PDMS thermal insulator is 1.48215mg/s under the solar radiation, while evaporation rate of the solution with rGO in room temperature without the light is 0.051367mg/s. Thus, the irradiation induced evaporation rate is 1.432037mg/s. With the evaporation surface of 15.2cm2, the true efficiency of photothermal conversion was calculated to be 61.55%. The result proves that the PDMS thermal insulator works perfectly for heat localization, raising both the evaporation rate and evaporation efficiency dramatically. Based on the information of IR image, the thermal insulator helps form a evaporation surface of 71℃, which is greatly higher than the group without thermal insulation. Such raise in surface temperature, in return, enhances the maximum voltage of our system, to an unprecedented level of more than 41mV (**Fig. 10C**). With the function of thermal insulator, the voltage has also been maintained at high level for a longer time. Even after the voltage test of 30mins, the open-circuit voltage is still higher than 30mV.

However, while the application of thermal insulator inside the system help enlarge and maintain the thermal gradient, it also restricts the ion path for the electrochemical process by covering the whole bottom surface of electrode. Such limitation of ion path results in the dramatic increase of internal resistance. As we can see from the images, although the total voltage has been increased to a large extent by thermal insulation, the maximum current of the system only reaches 700μA, due to the increased resistance (**Fig. 10D**). However, this disadvantage does not undermine the excellence of the system with PDMS insulator. Despite the smaller maximum current due to increase of internal resistance, the current at the steady state remains at 166μA, which is higher than the system merely with graphite-based rGO. Since the ion path has initially been restricted by the insulator, the electrochemical reaction, at the beginning, happen at a small rate, which is close to that of steady state. The concentration limit does not affect this system that much, that the current of this system does not experience a sharp drop like others. The thermal insulator also helps make the voltage sustainable at a high level, which also contributes to the higher current level at last.

The thermal insulator not only improves heat localization, but also leads to the highest voltage and considerable current. Such enhancement makes the thermoelectrochemical cell with graphite-based rGO and PDMS thermal insulator the best among all the mentioned systems, regarding of thermal gradient, voltage, current and evaporation efficiency. This thermoelectrochemical well with best performance in both interfacial evaporation and thermoelectrochemical reaction is, therefore, employed as our final system, tested for efficiency of energy conversion and design of scalable application.

3.8 Calculation of energy conversion efficiency of the best system

Our evaporation-enabled thermoelectrochemical cell allows high-efficient interfacial evaporation and thermoelectrochemical cell to work in the meantime, harvesting energy form solar radiation for water evaporation and generation of electricity. To figure out the best system of our evaporation enabled thermoelectrochemical cell, comparison of the four systems has been made, focusing on thermal evaporation performance, regarding of evaporation rate, true efficiency and thermal gradient. The result of the comparison is shown in the table below. (**Table 1.**)

Table 1. Comparison of Evaporation Performance

Evaporation System	True Evaporation	True Efficiency	Surface Temperature
paper-based rGO	1.28965g/s	53.31%	53℃
graphite foam	1.34392g/s	55.84%	60℃
graphite-based rGO	1.35928g/s	58.43%	67℃
graphite-based rGO with PDMS insulator	1.43204g/s	61.55%	71℃

It can be easily figured out from the data of **Table 1.**, the system with graphite-based rGO and PDMS insulator, has higher evaporation rate and true efficiency, and is, therefore, capable of converting more solar energy into heat and generating steam at a

higher rate. The enhancement of heat localization, achieved by PDMS thermal insulator, can further improve the temperature at the surface, which is beneficial for interfacial evaporation and thermoelectrochemical cell. Combined with the data of voltage and current of these four systems tested in previous experiments of thermoelectrochemical performance, the system with graphite-based rGO and PDMS insulator is selected as the best system among all. Hence, this system is selected for the following efficiency calculation.

The following experiments are carried out for efficiency calculation. The maximum electricity output power of our selected system has been tested by making comparisons of output power with different external resistances. The heat flow due to thermal gradient from the top to the bottom is considered as the energy source for electricity generation. The energy conversion efficiency of our thermoelectrochemical cell is calculated by dividing the total output power by the power of the heat flow from the top to the bottom.

In this experiment, we have, firstly, put the thermoelectrochemical cell with thermal insulator and graphite-based rGO exposed to solar radiation of 400mW/cm^2 to attain a considerable voltage level, and then connected to external resistances of different values with a resistance box. By comparing the output power of different resistances, the maximum output power is attained with the external resistance of 40Ω. The maximum output voltage is 18.75mV, when connected to the resistance of 40Ω. And the maximum output power, is therefore calculated to be 8.79μW, which is noted as P_{MAX}.

In the system with graphite-based rGO as evaporative surface and PDMS thermal insulator, the temperature at the evaporative surface and at the bottom have been detected to calculated ΔT for the heat flow. With a surface temperature of 71℃ and bottom temperature of 32℃ during evaporation, ΔT is calculated to be 39 K. The

distance between two graphite foam electrodes is measured to be 4.5 cm as the path for the heat flux to go through (Δx). As the host α-CDs in the employed low concentration range exerted negligible influence on the thermal conductivity (k) in the solution, we adopted the value of 0.6 $Wm^{-1}K^{-1}$ as reported by Hongyao Zhao. The heat flux during evaporation is calculated by the equation below (3-1):

$$q = -k\frac{\Delta T}{\Delta x} \tag{3-1}$$

Under the assumption that all of the heat transfers from the hot side to the cold side without thermal loss to ambient air, the heat flux can be calculated as 5.2×10^2 Wm^{-2}. The energy conversion efficiency is calculated by the following equation (3-2):

$$\eta = \frac{P_{MAX}}{qA} \tag{3-2}$$

In this equation, P_{MAX} is the maximum electricity output power as mentioned above, q is the heat flux due to thermal gradient, and A is the cross-sectional area of the electrolyte solution. With the P_{MAX} value of 8.79μW and the heat flow of 9.31×10^{-2}W, the energy conversion efficiency of our system is calculated to be 9.44×10^{-3}%. Such efficiency is much higher than the reported thermal efficiency of 3×10^{-3}% of the same electrolyte solution, due the enhancement of current based on the graphite foam electrodes.

A satisfactory energy conversion efficiency has been achieved by harvesting heat during interfacial evaporation for electricity generation, and improving the performance of both thermoelectrochemical cell and interfacial evaporation. In the meantime, our evaporation-enabled thermoelectrochemical cell reaches a Seebeck Coefficient of 1.45mV/K with inner convection, which is much higher than traditional thermoelectric materials. And since our system is liquid-based, thus flexible, whole

volume of solution can be divided into many separate tubes in series to generate a considerable voltage. More importantly, our system shares the same key factor, heat localization, with interfacial evaporation. In this case, all the strategies applied to enhance evaporation, can be directly used to optimize the performance of our system, which stands for great potential in future development.

In the meantime, it is worth noticing that, for other project studied in our research group, rGO and PDMS thermal insulator are also applied merely for interfacial evaporation, a much higher true efficiency is obtained than our data, reaching a maximum of 85%. The relatively smaller values of our evaporation data are due to our experimental equipment. While researchers on interfacial evaporation uses small container for experiment, to avoid severe heat dissipation, we use a beaker of 100mL, since large size of beaker is needed, if Pt wire electrodes and thermocouples need to be inserted into the container. More importantly, since solution level is lower than the beaker wall in our experiment, serious condensation of water vapor is happening along the evaporation process. The condensation of water vapor, to a larger scale, reduces the evaporation rate, since a great amount of vapor is trapped on the beaker wall, and then falls back into the solution, which should have been counted as mass loss if we applied the equipment for evaporation experiment. The condensation process will also undermine the surface temperature, by the falling of cooled water on the beaker wall. This is to claim that our system is still with great potential to be further enhanced, especially in the aspect of interfacial evaporation and heat localization. Even by simply exchanging our container with a smaller one with lower beaker wall, a better performance of evaporation, heat localization and efficiency can certainly be achieved.

The electrochemical efficiency of our system can also be further enlarged by avoiding the sharp current drop during electricity generation. We have herein designed a plan of thermoelectrochemical cell cycling to optimize the output power and efficiency in

practice, which can be employed by scalable applications.

3.9 Calculation of energy conversion efficiency for cycle plan

As shown in the former voltage and current, as the electricity generation continues, both the voltage and output power of the system will experience a sharp drop, since the thermal gradient as well as reactant concentration cannot be maintained. By breaking the above limits, the heat harvesting can be carried out with an unprecedented efficiency. We, therefore, design a thermoelectrochemical cell for practical application to realize the condition, where the solar energy can be merely applied to the initial state of thermoelectrochemical cell with high voltage.

In practice, although for an evaporation system, the area of solar evaporation is fixed, a series of thermoelectrochemical cells can be prepared for the same area and form a continuous cycle. During the cycle, each bottle of electrolyte is exposed to solar energy only during the initial stage, when there is the sharpest thermal gradient, thus considerable voltage can be maintained. After the initial stage, the bottle of electrolyte is replaced by a cooled bottle for solar radiation, and covered in room temperature to cool down. The heating up process of the electrolyte will form a concentration gradient inside the system, since the reduction and oxidation of I_3^- and I^- are thermal selective. When cooled down in room temperature without solar radiation, the concentration gradient can no longer be maintained, since the reaction balance will react towards the inverse direction, due to change of environmental temperature. This process will, consequently, lead to a continuous negative voltage, which add up to the total voltage by connecting the cooling thermoelectrochemical cell with the evaporating one. When the negative voltage falls back to zero, fresh water is added into the cell as a compensation for the mass loss during evaporation, and also to mix the electrolyte solution up again by the water

flux.

By setting up this cycle, we can always harvest heat with the thermoelectrochemical cell of best performance, and collect the negative voltage induced by the concentration change during the cooling process. This assures that, given the same amount of solar energy, more electricity can be generated via this cycle. We herein carry out an experiment to figure out to what extent the total amount of electric power can be increased, and to make sure that this cycle can be repeated with a satisfactory cycle performance. During the experiment, a beaker of 100mL electrolyte solution has been put into the system with graphite-based rGO evaporation surface and PDMS thermal insulator. The solution is firstly exposed to the solar radiation of 400mW/cm^2 for 15 mins to output power with the highest average voltage, connected to a resistance of 40Ω. Second, the solar radiation is covered, and the solution is cooled in room temperature for 40 mins to output electricity in the negative direction, until the voltage gradually falls back to zero. The solution is at last added the same amount of deionized water as its mass loss during the first two steps, and put in the room temperature to cool down for another 20mins. It is then exposed to solar radiation and repeat the whole cycle. In our work, the cycle has been repeated for three times to test the cycle performance. The voltage is collected during the first two steps of each cycle, and the result is shown below (**Fig. 11.**).

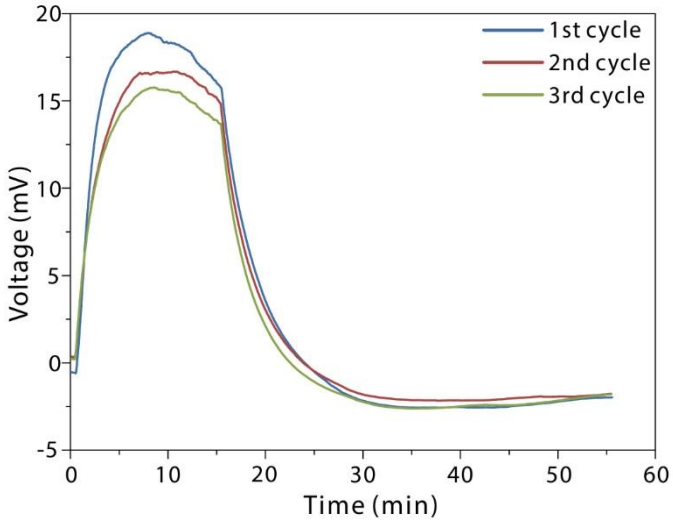

Fig. 11. The Cycle performance of voltage of thermoelectrochemical cell. By applying the cycle for electricity generation, the voltage can be maintained at considerable when exposed solar radiation. Both the positive voltage during radiation and negative voltage during cooling state have been collected for energy output.

It can be detected from figure above, by exposing the cooled solution to solar radiation, a higher maximum voltage can be attained, and maintained at considerable level during the whole evaporation process. After covering the solar radiation, the voltage drops dramatically due the decrease in thermal gradient, and then turns into negative voltage, due to the balance of reactant concentration. The negative voltage can reach a maximum absolute value of 3mV, which is helpful to increase the total voltage. The total output power during the first two steps is calculated as the table below. (**Table 2.**)

Table 2. Improvement of Output Power in Cycle Plan

Cycle Number	Average Power	Total Energy	Percentage Improvement
Cycle 1	2.12×10^{-6}W	6.99×10^{-3}J	52.13%
Cycle 2	1.92×10^{-6}W	6.35×10^{-3}J	38.23%
Cycle 3	1.69×10^{-6}W	5.57×10^{-3}J	21.18%

As shown in (**Table 2.**), The first cycle, second cycle and third cycle achieves an average output power of 2.12×10^{-6}W, 1.92×10^{-6}W and 1.69×10^{-6}W, respectively. Since the electricity is collected during the first 55 mins for each run, the total output energy is calculated above. As we have tested in the former test of electricity output at steady sate, the electricity output power is 5.103×10^{-6}W. The total electricity output for steady state is 4.592×10^{-3}J. As a result, the first, second and third cycle has increased the total electricity generation by 52.13%, 38.23% and 21.18% respectively. In this case, our cycle has effectively raised the efficiency of electricity generation, by maintaining voltage of a high level and collecting the extra energy during the cooling process. The result can, in the meantime, state that our thermoelectrochemical cell is repeatable, and that the total energy generation can still

be increased to a large extent, even our cycle process has been repeated.

This experiment introduces a cycle plan, which can be applied to scalable application to increase the heat harvesting efficiency to a large scale. Apart from the cycle, our thermoelectrochemical cell system, enabled by interfacial evaporation can be further enhanced by many other methods, due to its flexibility afforded by its liquid state. Strategies like connecting cells in series to increase voltage, and enlarging the electrode surface to enlarge current can all be adopted to increase the efficiency further. With these strategies, our thermoelectrochemical cell is believed to harvest heat at a higher efficiency than calculated above. Our thermoelectrochemical cell enabled by evaporation, is therefore, a perfect candidate, for scale-up application to harvest waste heat during water desalination.

Chapter 4. Conclusion

To relieve the global lack of drinkable water and shortage of energy resources, we have firstly demonstrated an evaporation enabled thermoelectrochemical cell, to harvest heat into electricity during the interfacial evaporation process. Our thermoelectrochemical cell is driven by the thermal gradient from the top to bottom. The half reactions of the redox couple in our electrolyte is highly thermal-selective, thus an open-circuit voltage can be achieved, when exposed to solar radiation. Among all the thermoelectrochemical electrolyte, we finally determine to apply the electrolyte based on I^-/I_3^- to our system, due to its hypotoxicity and low-cost. α-CD and KCl have been added into the electrolyte solution to sharpen the concentration difference and improve the electric conductivity of solution.

To achieve a better performance of heat localization and improve the steam generation efficiency during evaporation, several strategies have been investigated to optimize

our evaporation performance as well as thermoelectrochemical performance. Paper-based rGO, graphite foam, graphite-based rGO have been compared as candidate for evaporation surface materials, regarding of solar absorption, evaporation efficiency and surface temperature. The thermal insulator, made of PDMS, has also been introduced into the system, to enhance heat localization and to, consequently, enlarge the thermal gradient for higher output voltage and evaporation performance. The system of graphite-based rGO as electrode and evaporation surface with PDMS thermal insulator has finally been selected as the best system, for its outstanding performance in evaporation rate, steam generation efficiency, surface temperature and thermoelectrochemical performance of the system.

Experiments have then been carried out with the above selected system to test the energy conversion efficiency of our system. With maximum electricity output power with an external resistance of 40Ω is divided by the power of heat flow due to thermal gradient during evaporation. The result reveals that, the heat harvesting of thermoelectrochemical cell has converted part of the thermal energy into output electricity with a thermal efficiency of $9.44 \times 10^{-3}\%$. Compared to the thermoelectrochemical cell of the same electrolyte used as a thermoelectric device, which has a thermal efficiency of $3 \times 10^{-3}\%$, our system exhibits much higher energy conversion efficiency due to the enhancement of current based on graphite foam electrodes.

We have then come up with a cycle plan for scalable application in practice, which can further enlarge the total energy, and enhance the electricity generation efficiency. By setting up the cycle of heating up-cooling down-adding fresh water, the thermoelectrochemical cell is assured to sustain electricity generation at a considerable voltage level. The first cycle, second cycle and third cycle has increased the electricity generation efficiency by 52.13%, 38.23%, 21.18% respectively, compared to the electricity output power at steady-state evaporation. The drop of

improved efficiency is due the heating up of the bulk water, since in our experiment, the solution has not been cooled down for sufficient time. However, the results still reveal that our thermoelectrochemical is repeatable, and the cycle plan has a good cycle performance in enhancing the electricity generation efficiency.

In the meantime, since our thermoelectrochemical cell is of liquid-state and flexible, plenty of other methods can be applied to enhance the energy output, such as separating the solution into difference small tubes and connecting all the tubes in series to multiply the voltage. The hydrophilicity and thermal insulation of evaporation surface, which are investigated by many interfacial evaporation research group, can also be applied to increase our system. Moreover, since our evaporation enabled thermoelectrochemical cell shares the same key factor, heat localization, with interfacial evaporation, all the research development in interfacial evaporation can be directly applied to our system to further enhance the evaporation efficiency and thermoelectrochemical performance.

However, our experiments also have drawbacks to overcome. One of the most important problem is the oversize of our experimental equipment. The beaker to contain electrolyte solution is too huge for test of evaporation, while the beaker wall has also caused serious steam condensation, which severely undermines our evaporation efficiency. This steam condensation has also undermined the thermal gradient, by forming the stream of cooled water from the beaker wall to the evaporation surface. We should later on design the experimental equipment with smaller, based on the design of container used in interfacial evaporation research project. The replacement of the equipment of smaller size is believed to enhance both the evaporation performance and thermoelectrochemical performance of our system.

Besides, our experiments are all carried out with the solar radiation of 400mW/cm^2 to attain higher evaporation rate and to form a sharp thermal gradient in a shorter time.

Experiments with 1 sun solar radiation should also been carried out to test both the evaporation performance and thermoelectrochemical performance, to figure out whether our evaporation enabled thermoelectrochemical has the potential of scalable application in common solar illumination. The 1 sun solar radiation may fail to form a sharp temperature difference between the top and bottom like current thermal gradient, which can lead to decrease of open-circuit voltage. However, the difference of evaporation rate between the group with open-circuit and the group with electricity output may also become smaller in the meantime, which leads to increase the energy conversion efficiency.

In summary, our work successfully combined the high-efficient interfacial evaporation and thermoelectrochemical cell to realize electricity generation enabled by evaporation. By applying this bifunctional heat harvesting system, we have achieved a thermal efficiency of $9.44 \times 10^{-3}\%$, which is much higher than the data reported by other research of the same type of thermoelectrochemical cell. Several strategies have been investigated to improve the evaporation and thermoelectrochemical performance, and a suitable system with high performance was obtained. A cycle plan has been brought up for improvement in scalable application. Enhancements, like replacement of electrolyte container with a smaller one can be applied to further improve our evaporation and thermoelectrochemical performance. Parallel experiments under the solar illumination of 100mW/cm^2 should also be done to test the performance of our system without solar concentration.

REFERENCE

[1]. Boyle, G. Renewable energy: power for a sustainable future[M]. Taylor & Francis, 1997.

[2]. Hoffert, M. I.,Caldeira, K.,Benford, G., etc. Advanced technology paths to global climate stability: energy for a greenhouse planet[J]. Science, 2002, 298 (5595): 981-987.

[3]. Johansson, T. B. Renewable energy: sources for fuels and electricity[M]. Island press, 1993.

[4]. Turner, J. A. A realizable renewable energy future[J]. Science, 1999, 285 (5428): 687-689.

[5]. Cartlidge, E. Saving for a rainy day[J]. Science, 2011, 334 (6058): 922-924.

[6]. Elimelech, M.,Phillip, W. A. The future of seawater desalination: energy, technology, and the environment[J]. Science, 2011, 333 (6043): 669-671.

[7]. Gupta, M. K.,Kaushik, S. C. Exergy analysis and investigation for various feed water heaters of direct steam generation solar–thermal power plant[J]. Renewable Energy, 2010, 35 (6): 1228-1235.

[8]. Scuderi, V.,Impellizzeri, G.,Romano, L., etc. An enhanced photocatalytic response of nanometric TiO2 wrapping of Au nanoparticles for eco-friendly water

applications[J]. Nanoscale, Oct 07, 2014, 6 (19): 11189-11195.

[9]. Fh, V. D. H.,Bonthuis, D. J.,Stein, D., etc. Power generation by pressure-driven transport of ions in nanofluidic channels[J]. Nano Letters, 2007, 7 (4): 1022-1025.

[10].Li, C.,Liu, K.,Liu, H., etc. Capillary driven electrokinetic generator for environmental energy harvesting[J]. Materials Research Bulletin, 2017, 90 81-86.

[11].Xue, G.,Xu, Y.,Ding, T., etc. Water-evaporation-induced electricity with nanostructured carbon materials[J]. Nature Nanotechnology, May, 2017, 12 (4): 317-321.

[12].Dhiman, P.,Yavari, F.,Mi, X., etc. Harvesting energy from water flow over graphene[J]. Nano Letters, Aug 10, 2011, 11 (8): 3123-3127.

[13].Wang, Z.,Liu, Y.,Tao, P., etc. Bio-inspired evaporation through plasmonic film of nanoparticles at the air-water interface[J]. Small, Aug 27, 2014, 10 (16): 3234-3239.

[14].Liu, Y.,Yu, S.,Feng, R., etc. A bioinspired, reusable, paper-based system for high-performance large-scale evaporation[J]. Advanced Materials, May 06, 2015, 27 (17): 2768-2774.

[15].Liu, Y.,Lou, J.,Ni, M., etc. Bioinspired Bifunctional Membrane for Efficient Clean Water Generation[J]. ACS Applied Materials & Interfaces, Jan 13, 2016, 8 (1): 772-779.

[16].Zhou, L.,Tan, Y.,Wang, J., etc. 3D self-assembly of aluminium nanoparticles for plasmon-enhanced solar desalination[J]. Nature Photonics, 2016.

[17].Zhou, L.,Tan, Y.,Ji, D., etc. Self-assembly of highly efficient, broadband plasmonic absorbers for solar steam generation[J]. Science Advances, 2016, 2 (4): e1501227.

[18].Lou, J.,Liu, Y.,Wang, Z., etc. Bioinspired Multifunctional Paper-Based rGO Composites for Solar-Driven Clean Water Generation[J]. ACS Applied Materials & Interfaces, Jun 15, 2016, 8 (23): 14628-14636.

[19].Ghasemi, H.,Ni, G.,Marconnet, A. M., etc. Solar steam generation by heat

localization[J]. Nature Communications, Jul 21, 2014, 5 4449-4455.

[20].Hu, X.,Xu, W.,Zhou, L., etc. Tailoring Graphene Oxide-Based Aerogels for Efficient Solar Steam Generation under One Sun[J]. Advanced Materials, 2017, 29 (5).

[21].Hertz, H. G.,Ratkje, S. K. Theory of thermocells[J]. Journal of the Electrochemical Society, 1989, 136 (5): 1698-1704.

[22].Hu, R.,Cola, B. A.,Haram, N., etc. Harvesting waste thermal energy using a carbon-nanotube-based thermo-electrochemical cell[J]. Nano Letters, 2010, 10 (3): 838-846.

[23].Kang, T. J.,Fang, S.,Kozlov, M. E., etc. Electrical Power From Nanotube and Graphene Electrochemical Thermal Energy Harvesters[J]. Advanced Functional Materials, 2012, 22 (3): 477–489.

[24].Qian, W.,Cao, M.,Xie, F., etc. Thermo-Electrochemical Cells Based on Carbon Nanotube Electrodes by Electrophoretic Deposition[J]. Nano-Micro Letters, 2016, 8 (3): 240-246.

[25].Abraham, T. J.,MacFarlane, D. R.,Pringle, J. M. High Seebeck coefficient redox ionic liquid electrolytes for thermal energy harvesting[J]. Energy & Environmental Science, 2013, 6 (9): 2639-2646.

[26].Lazar, M. A.,Al-Masri, D.,MacFarlane, D. R., etc. Enhanced thermal energy harvesting performance of a cobalt redox couple in ionic liquid-solvent mixtures[J]. Physical chemistry chemical physics : PCCP, Jan 21, 2016, 18 (3): 1404-10.

[27].Abraham, T. J.,MacFarlane, D. R.,Baughman, R. H., etc. Towards ionic liquid-based thermoelectrochemical cells for the harvesting of thermal energy[J]. Electrochimica Acta, 2013, 113 87-93.

[28].Tuza, K.,Jicsinszky, L.,Sohajda, T., etc. Synthesis of modified cyclic and acyclic dextrins and comparison of their complexation ability[J]. Beilstein Journal of Organic Chemistry, 2014, 10 (10): 2836-2843.

[29].Hasan, S. W.,Said, S. M.,Sabri, M. F., etc. High Thermal Gradient in

Thermo-electrochemical Cells by Insertion of a Poly(Vinylidene Fluoride) Membrane[J]. Scientific reports, Jul 06, 2016, 6 29328.

[30].Abraham, T. J.,Tachikawa, N.,MacFarlane, D. R., etc. Investigation of the kinetic and mass transport limitations in thermoelectrochemical cells with different electrode materials[J]. Physical chemistry chemical physics : PCCP, Feb 14, 2014, 16 (6): 2527-32.

[31].Im, H.,Kim, T.,Song, H., etc. High-efficiency electrochemical thermal energy harvester using carbon nanotube aerogel sheet electrodes[J]. Nature communications, Feb 03, 2016, 7 10600.

[32].Anari, E. H.,Romano, M.,Teh, W. X., etc. Substituted ferrocenes and iodine as synergistic thermoelectrochemical heat harvesting redox couples in ionic liquids[J]. Chemical communications, Jan 14, 2016, 52 (4): 745-8.

ACKNOWLEDGEMENT

Upon finishing this thesis, I would like to express my great gratitude towards all those who have supported and encouraged me.

First and foremost, my hearty thanks go to my supervisors, Professor Tao Deng and Professor Wen Shang, who have given me insightful suggestions and constant encouragement both in my study and in my life. Furthermore, Professor Tao Deng, as both my research advisor and course teacher, has enlightened my passion for research in materials science, by unfolding the fancy research achievements before my eyes and revealing the scientific fundamentals underneath. His advice and assistance during my graduate application has refreshed my cognition of materials research and what I should do in my future doctoral study. His self-discipline and academic pursuit has set a perfect example for me to imitate and chase after during the rest of my academic career.

Also, I owe my thanks to Mr. Qingchen Shen, who has guided me in the field of research work in both my undergraduate thesis project and my research project in junior year. His persistence, hardworking has rebuilt my academic attitude in a more rigorous manner. Without his selfless help and heated discussion with me, this thesis project can hardly be completed.

Besides, I want to express my thanks to my parents, who always support me and encourage me. They give me the freedom of making all my big decisions, and in the meantime, respect, trust and unconditionally support my decisions and career plan. Without their trust and support, I can never become anyone tough and independent. Their care and support motivate me to move on and to become a better man.

Finally, I am so grateful to my girlfriend, Luyi Chen, who has accompanied me for almost my whole campus life. She has brought me more possibilities of life, a different cognitive perspective to the world, and the motivation of self-improvement. As what I have said to her: I was born carbon. The stress and pressures make me firm. The difficulties and sufferings make me carved. She is my sun, she makes me shine, like diamonds.

Thank you all very much.